Novel Products from Reactions of $Li[(\mu\text{-}CO)(\mu\text{-}RS)Fe_2(CO)_6]$ Salts with Ethoxyacetylene†

Dietmar Seyferth,* Jeffrey B. Hoke, and John C. Dewan

Department of Chemistry, Massachusetts Institute of Technology, Cambridge, Massachusetts 02139

Peter Hofmann* and Michael Schnellbach

Anorganisch-Chemisches Institut der Universität München, Lichtenbergstrasse 4, D-85747 Garching, Germany

Received January 14, 1994®

Reactions of $Li[(\mu\text{-}CO)(\mu\text{-}RS)Fe_2(CO)_6]$ salts with ethoxyacetylene followed by reaction of the anionic intermediate thus generated with acetyl or benzoyl chloride gave an $Fe_2(CO)_6$ complex that contained the thiolate ligand as well as a novel resonance-stabilized bridging vinylcarbene ligand which incorporated the acetylene and an original CO ligand that may be written as $-C(OEt)=CHC(O_2CR^1)= \leftrightarrow =C(OEt)CH=C(O_2CR^1)-$. The structure of the complex in which R = *t*-Bu and $R^1 = CH_3$ was determined by X-ray diffraction. Extended Hückel MO calculations for a model system, $Fe_2(CO)_6(\mu\text{-}SH)(\mu\text{-}C_3H_3)$, led to its description in terms of an ideally delocalized C_3 bridge coupled to the iron atoms of the $(\mu\text{-}HS)Fe_2(CO)_6$ unit by two strong σ-bonds and by moderate π-back-bonding. Protonation of the anionic intermediate with trifluoroacetic acid gave the α,β-unsaturated bridging acyl complexes $(\mu\text{-}EtOC(=CH_2)C=O)(\mu\text{-}RS)Fe_2(CO)_6$ (R = *t*-Bu, Et). The X-ray crystal structure of the complex in which R = *t*-Bu was determined. These complexes lost CO in THF solution at room temperature, giving $(\mu\text{-}EtOC=CH_2)(\mu\text{-}RS)Fe_2(CO)_6$.

Introduction

As reported in a previous paper,[1] reactions of alkyl- and arylacetylenes with triethylammonium salts of $[(\mu\text{-}CO)(\mu\text{-}RS)Fe_2(CO)_6]^-$ anions (**1**) yield as major products bridging σ,π-olefin complexes of type **2** (eq 1). The

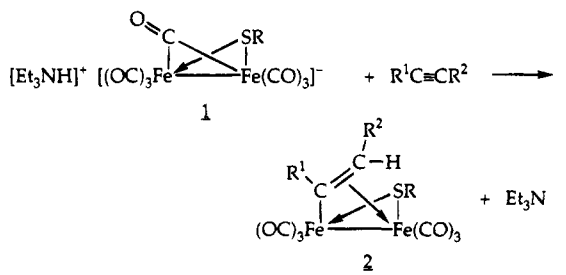

1 2 (1)

isolation of neutral $\mu\text{-}\sigma,\pi$-vinyl rather than anionic alkynyl or vinyl complexes is due to the facile, *in situ* protonation of the intermediate vinylic anion **3** by the

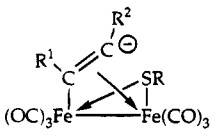

3

acidic Et_3NH^+ ion. It might be expected that, in the absence of the triethylammonium ion, the transient vinyl anion **3** would be sufficiently long-lived to undergo reaction with diverse electrophiles, E^+, that are added to the reaction mixture, giving the products of type **4**.

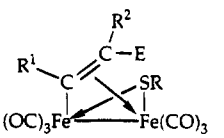

4

It was the purpose of this investigation to examine this possibility and, if anions of type **3** indeed were trappable intermediates, to explore their chemistry. The present paper deals with reactions of $Li[(\mu\text{-}CO)(\mu\text{-}RS)Fe_2(CO)_6]$ salts with ethoxyacetylene. A later paper will report details of the reactions of these salts with α,β-unsaturated acetylenes.[2] In both cases the observed results were not the expected ones. Instead, $Fe_2(CO)_6$ complexes with bridging ligands that contained not only the acetylene used but also a CO ligand and even the RS ligand were obtained. For one class of these novel compounds (**5**) an X-ray structure determination reveals the formation of delocalized C_3R_3 units, which are formed by alkyne–CO coupling under acylating conditions. They can be formally regarded as ring-opened cyclopropenium cations symmetrically bridging an $Fe_2(CO)_6(\mu\text{-}RS)^-$ fragment in a $\mu\text{-}\eta^1\text{:}\eta^1$ fashion. The electronic structure of these complexes **5**, which turn out to be closely related to "Fischer-type" carbene complexes, is another subject of this work.

† Dedicated to Professor Helmut Werner, with all best wishes, on the occasion of his 60th birthday.

® Abstract published in *Advance ACS Abstracts,* June 1, 1994.

(1) Seyferth, D.; Hoke, J. B.; Womack, G. M. *Organometallics* **1990,** *9,* 2662.

(2) For a preliminary communication see: Seyferth, D.; Hoke, J. B.; Dewan, J. C. *Organometallics* **1987,** *6,* 895.

0276-7333/94/2313-3452$04.50/0

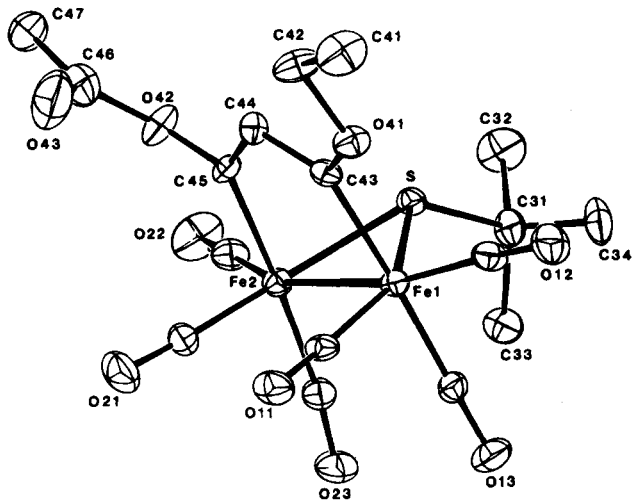

Figure 1. ORTEP diagram of **5a** showing 20% probability thermal ellipsoids.

Results and Discussion

The reactions of ethoxyacetylene with the Li[(μ-CO)(μ-RS)$Fe_2(CO)_6$] salts (R = *t*-Bu, Et) were carried out in THF at room temperature. In the expectation that an anionic $Fe_2(CO)_6$ complex had been formed, an acid chloride ($CH_3C(O)Cl$ or $C_6H_5C(O)Cl$) was added to the reaction mixture. Over a period of several hours a cherry red reaction mixture resulted. After removal of the solvent, filtration chromatography served to isolate a single product in each case as an air-stable, red solid in good yield.

Elemental analysis of these products was in agreement with a composition including the $Fe_2(CO)_7SR$ moiety, ethoxyacetylene, and the respective R'C(O) unit. An X-ray crystal structure determination was carried out for the product of the reaction of EtOC≡CH with Li[(μ-CO)(μ-*t*-BuS)$Fe_2(CO)_6$] and $CH_3C(O)Cl$. An ORTEP plot showing 20% probability thermal ellipsoids and the atom-labeling scheme is shown in Figure 1. A line drawing of these products is shown in eq 2, which shows also the other products of type **5** which were prepared.

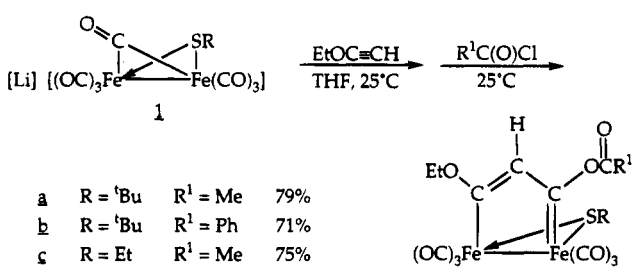

(2)

In these reactions a CO ligand has been incorporated into the bridging organic ligand. The intermediate in solution, prior to the addition of the acid chloride, must have been **6**. Complexes of type **5** are interesting in that

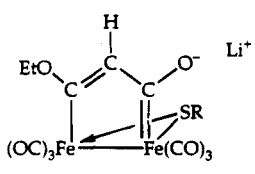

Table 1. Relevant Bond Distances (Å) and Angles (deg) for 5a

Fe(1)–Fe(2)	2.638(2)	C(42)–C(41)	1.515(13)
Fe(1)–S	2.252(2)	C(45)–O(42)	1.363(9)
Fe(2)–S	2.256(3)	O(42)–C(46)	1.319(14)
Fe(1)–C(43)	1.976(8)	C(46)–C(47)	1.477(16)
Fe(2)–C(45)	1.967(8)	C(46)–O(43)	1.223(14)
C(43)–C(44)	1.392(11)	S–C(31)	1.875(9)
C(44)–C(45)	1.365(11)	C(31)–CH_3 (mean)	1.558
Fe(1)–C(44)	3.010	Fe(1)–CO (mean)	1.781
Fe(2)–C(44)	2.997	Fe(1)C–O (mean)	1.140
Fe(2)–C(43)	3.169	Fe(2)–CO (mean)	1.787
Fe(1)–C(45)	3.157	Fe(2)C–O (mean)	1.136
C(43)–O(41)	1.318(9)	O(41)–C(42)	1.501(11)
S–Fe(1)–Fe(2)	55.4(1)	O(42)–C(46)–C(47)	115.6(12)
Fe(2)–S–Fe(1)	71.3(1)	O(43)–C(46)–C(46)	124.6(14)
Fe(1)–Fe(2)–S	54.3(1)	O(42)–C(45)–C(44)	118.4(8)
S–Fe(1)–C(43)	84.9(3)	C(45)–C(44)–C(43)	115.4(8)
S–Fe(2)–C(45)	82.3(3)	C(44)–C(43)–Fe(1)	125.8(6)
Fe(1)–S–C(31)	120.2(3)	C(44)–C(43)–O(41)	119.0(8)
Fe(2)–S–C(31)	120.9(3)	C(43)–O(41)–C(42)	119.8(7)
Fe(2)–C(45)–C(44)	127.3(6)	O(41)–C(42)–C(41)	105.0(8)
Fe(2)–C(45)–O(42)	114.3(6)	O(41)–C(43)–Fe(1)	115.2(6)
C(45)–O(42)–C(46)	128.5(9)	C(43)–Fe(1)–Fe(2)	85.8(2)
O(42)–C(46)–O(43)	119.5(13)	C(45)–Fe(2)–Fe(1)	85.5(3)

two resonance forms can be drawn for the vinylcarbene bridge (eq 3).

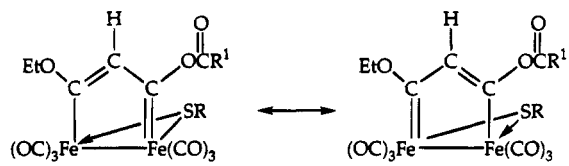

(3)

The basic structure of **5a** consists of a diiron hexacarbonyl core linked in a butterfly arrangement by the thiolate and delocalized vinylcarbene bridges. The thiolate bridge itself is nearly perfectly symmetrical, as evidenced by the Fe(1)–S and Fe(2)–S distances of 2.252(2) and 2.256(3) Å as well as the Fe(2)–Fe(1)–S and Fe(1)–Fe(2)–S angles of 55.4(1) and 54.3(1)°, respectively. (Important bond distances and angles are given in Table 1). The *tert*-butyl group occupies an equatorial (as opposed to an axial) position on the bridging sulfur atom, thereby minimizing steric interactions with the neighboring vinylcarbene bridge. While the iron–sulfur distances are standard for thiolate-bridged diiron complexes,[3] the C(31)–S bond of 1.875(9) Å is slightly longer than typical carbon–sulfur single bonds of 1.815(1) Å,[4] and this indicates some delocalization of electron density out of the thiolate bridge into the diiron core.

Delocalization of electron density throughout the vinylcarbene bridge is likewise evident. The similar C(43)–C(44) and C(44)–C(45) bonding distances of 1.392(11) and 1.365(11) Å, respectively, are considerably shorter than typical carbon–carbon single bonds of 1.541(3) Å[4] but, conversely, slightly longer than typical carbon–carbon double bonds of 1.337(6) Å.[4] Likewise, the nearly equivalent Fe(2)–C(45) and Fe(1)–C(43) distances of 1.967(8) and 1.976(8) Å are in the range of known, related iron carbene or carbene-like (i.e., μ-vinyl,

(3) (a) Weber, H. P.; Bryan, R. F. *J. Chem. Soc. A* **1967**, 182. (b) Dahl, L. F.; Wei, C.-H. *Inorg. Chem.* **1963**, *2*, 328. (c) Henslee, W.; Davis, R. E. *Cryst. Struct. Commun.* **1972**, *4*, 403. (d) Seyferth, D.; Womack, G. B.; Song, L.-C.; Cowie, M.; Hames, B. W. *Organometallics* **1983**, *2*, 928. (e) Seyferth, D.; Womack, G. B.; Dewan, J. C. *Organometallics* **1985**, *4*, 398.

(4) *International Tables for X-ray Crystallography*; MacGillavry, C. M., Rieck, G. D., Eds.; Kynoch Press: Birmingham, England, 1974; Vol. 3, p 276.

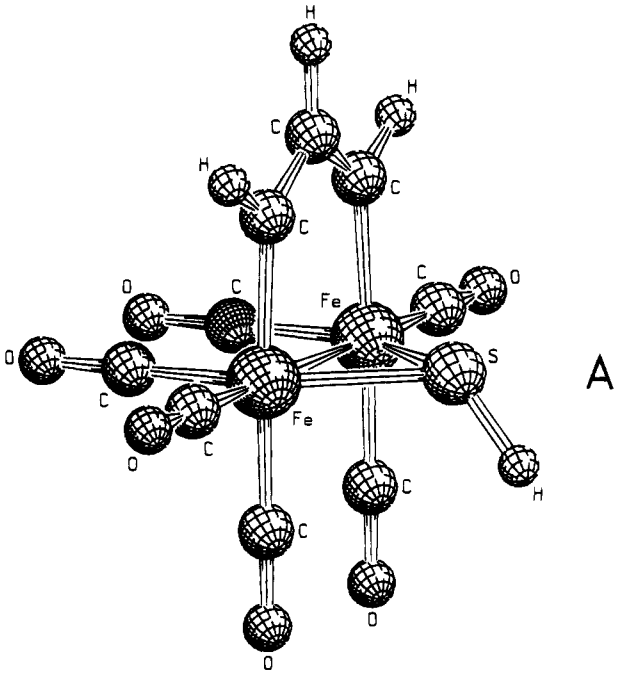

A

μ-acetylide, μ-acyl) systems.[3e,5,6] Furthermore, the symmetry of the vinylcarbene–diiron ring with respect to an orthogonal plane bisecting the angle C(43)–C(44)–C(45) is easily seen in the Fe(2)–C(45)–C(44) and Fe(1)–C(43)–C(44) angles of 127.3(6) and 125.8(6)° as well as the C(45)–Fe(2)–Fe(1) and C(43)–Fe(1)–Fe(2) angles of 85.5(3) and 85.8(2)°, respectively. In fact, the electron delocalization in the ring is so pronounced that the largest deviation from a plane defined by Fe(1), Fe(2), C(43), C(44), and C(45) is only 0.0346(1) Å for C(43). Inclusion of O(41) and O(42) with these five ring atoms defines a plane with a largest deviation of 0.0799(1) Å, and therefore, double-bond character extends to these oxygen atoms as well. Fischer-type alkoxy- and (acyloxy)carbenes display considerable carbon–oxygen double–bond character,[6a,7] and the observed C(45)–O(42) and C(43)–O(41) bond distances of 1.363(9) and 1.318(9) Å, respectively, are indicative of increased bond order.

In order to obtain a somewhat more quantitative description of the electronic structure and bonding pattern for **5a** and for its congeners, especially in relation to the observed solid-state structure described above, we have performed MO calculations of the extended Hückel type[8a,b] for a simplified model of systems **5**, namely for $Fe_2(CO)_6(\mu\text{-SH})(\mu\text{-}C_3H)$, shown in **A**. In the context of the potential "aromaticity" of some metallacycles, the extended Hückel HOMO–LUMO gap and the character of the frontier orbitals of **5a** have been reported recently,[8c] but no further details of its electronic structure were given. In **A**, the bridging C_3 and the bridging sulfur unit only carry hydrogens for simplicity. For all calculated structures of unsubstituted **A**, C_s symmetry is retained; bond distances and angles for the idealized geometry as represented in **A** are given in the Experimental Section. In a simplified manner, complexes of type **5** can be regarded as substituted M–M-bonded $M_2(CO)_{10}$ complexes with two distorted-octahedral iron centers and two pairs of *cis* carbonyls replaced by C_3R_3 and the SR bridges. For electron-counting purposes we can take the SR (SH in **A**) units as monoanions and the bridging C_3R_3 moieties as cations. This leaves us with the neutral bimetallic fragment $Fe_2(CO)_6$ (d^8–d^8), the electronic structure and bonding capability of which have been described in detail by Thorn and Hoffmann,[9] and we will make use of their results (*vide infra*). A μ-SR^- group, according to **B**, provides three (canonical) lone-pair MOs, which are,

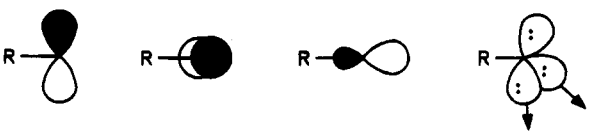

B C

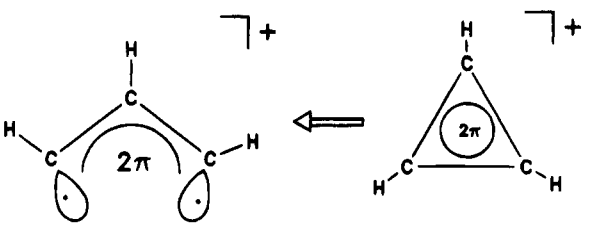

D E

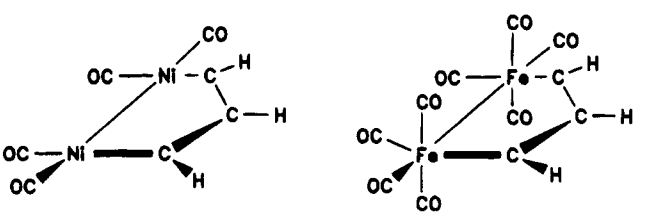

F G

of course, equivalent to the more familiar three localized nonbonding orbitals shown in **C**. Therefore, SR^- can function as a two-electron donor to each iron center. A

(5) (a) Krüger, C.; Tsay, Y. H.; Grevels, F. W.; von Gustorf, E. K. *Isr. J. Chem.* **1972**, *10*, 210. (b) Hickey, J. P.; Huffman, J. C.; Todd, L. J. *Inorg. Chim. Acta* **1978**, *28*, 77. (c) Schrauzer, G. N.; Rabinowitz, H. N.; Frank, J. K.; Paul, I. C. *J. Am. Chem. Soc.* **1970**, *92*, 213. (d) Andrianov, V. G.; Struchkov, Y. T. *Chem. Commun.* **1968**, 1590. (e) Aime, S.; Milone, L.; Sappa, E.; Tiripicchio, A.; Camellini, M. T. *J. Chem. Soc., Dalton Trans.* **1979**, 1155. (f) Hoffmann, K.; Weiss, E. *J. Organomet. Chem.* **1977**, *128*, 225. (g) Nakamura, Y.; Bachmann, K.; Heimgartner, H.; Schmid, H.; Daly, J. J. *Helv. Chim. Acta* **1978**, *61*, 589.

(6) (a) Schubert, U. In *Transition Metal Carbene Complexes*; Dötz, K. H., Fischer, H., Hofmann, P., Kreissl, F. R., Schubert, U., Weiss, K., Eds.; Verlag Chemie: Weinheim, Germany, 1983; pp 73–112. (b) Lindley, P. F.; Mills, O. S. *J. Chem. Soc. A* **1969**, 1279. (c) Patel, H. A.; Fischer, R. G.; Carty, A. J.; Palenik, G. J. *J. Organomet. Chem.* **1973**, *60*, C49. (d) Churchill, M. R. In *Perspectives in Structural Chemistry*; Dunitz, J. D., Ibers, J. A., Eds., Wiley: New York, 1970, Vol. 3, pp 128.

(7) (a) Fischer, E. O. *Adv. Organomet. Chem.* **1976**, *14*, 1. (b) Fischer, E. O. *Pure Appl. Chem.* **1972**, *30*, 353. (c) Cotton, F. A.; Lukehart, C. M. *Prog. Inorg. Chem.* **1972**, *16*, 487.

(8) (a) Hoffmann, R. J. *Chem. Phys.* **1963**, *39*, 1397. (b) Hoffman, R.; Lipscomb, W. N. *J. Chem. Phys.* **1962**, *36*, 2179, 3489. (c) Chamizo, J. A.; Morgando, J.; Sosa, P. *Organometallics* **1993**, *12*, 5005. 3D contour plots of the HOMO and LUMO given in Figure 3 are shown in this paper.

(9) Thorn, D. L.; Hoffmann, R. *Inorg. Chem.* **1978**, *17*, 126.

bridging μ-$C_3R_3^+$ (or μ-$C_3H_3^+$ in **A**) ligand, on the other hand, is nothing more than a ring-opened or bond-stretched cyclopropenium cation, as displayed in **D**. It can provide two σ-type donor orbitals with a total of two electrons (the electrons of a σ-bonding pair of the former C–C bond) to both iron atoms. Additionally, it has a delocalized π-system of the allyl cation type holding two π electrons. The orbitals of the ring-opened cyclopropenium cation **D**, and the way in which they are derived from the familiar valence MOs of the D_{3h} cyclopropenium ion **E**, have also been described in the literature,[10] and we will refer to this work of Jemmis and Hoffmann in the following. Interestingly, these authors have already discussed bonding patterns of ring-opened (or bond-stretched) cyclopropenium units atop binuclear or polynuclear metal fragments. Among other cases, they studied the hypothetical complexes $Ni_2(CO)_4(\mu\text{-}C_3H_3)$ (**F**) and $Fe_2(CO)_8(\mu\text{-}C_3H_3)$ (**G**). For the Ni compound a planar Ni_2C_3 five-membered ring structure as in **5** and **A** was concluded to be less stable than its geometric isomer with the ring-opened C_3H_3 rotated by 90° and bisecting the Ni–Ni vector. The hypothetical system **G** was only briefly mentioned in relationship to "di-σ"-bonded acetylene complexes[11] but was not discussed further. Its structural relationship to complexes **5** and their model **A** (two CO ligands instead of a μ-SR group) is obvious, although the electron counts of **A** and **G** differ. The overall electron count of 17 valence electrons for each Fe in **A** and complexes **5** formally requires an Fe–Fe single bond in order to accomplish an 18-electron configuration at both metal centers.

Therefore, the simplest way to describe the bonding pattern for **A** or the real compounds **5** is to start out from an $Fe_2(CO)_6$ fragment with the sawhorse (C_{2v}) geometry **H**. As detailed by Thorn and Hoffmann,[9] the

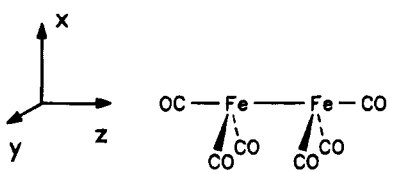

H

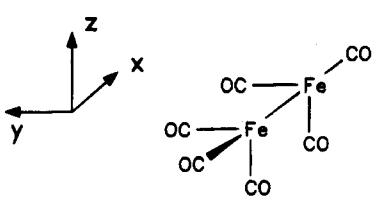

I

valence and frontier orbitals of **H**, which are essential for the bonding of additional ligands to this dimetallic unit, can be readily obtained by symmetrically assembling two "octahedral" $Fe(CO)_3$ building blocks and by relaxing the D_{3h} $Fe_2(CO)_6$ to the C_{2v} geometry shown in **H**. Alternatively, we can derive the valence MOs of a sawhorse $Fe_2(CO)_6$ by formally removing four *cis*

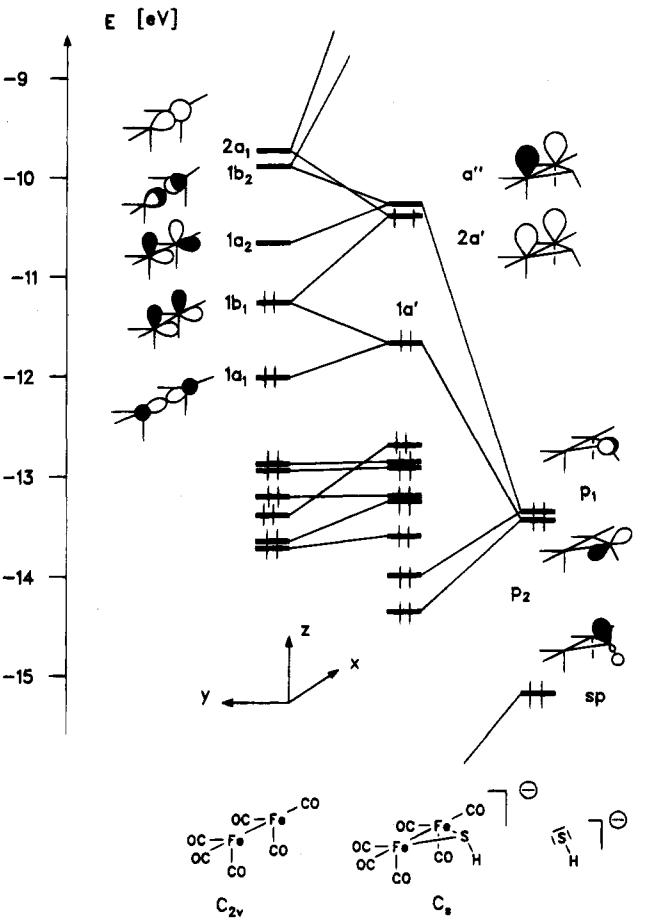

Figure 2. Orbital interaction diagram for $Fe_2(CO)_6(\mu\text{-}SH)^-$ between a sawhorse-type $Fe_2(CO)_6$ group (C_{2v}, oriented as shown in **I**) and a μ-SH^- group. Only the relevant valence orbitals of the metal fragment are sketched with their metal contributions. For contour diagrams of $Fe_2(CO)_6(\mu\text{-}SH)^-$ levels a'', 2a', and 1a' see Figure 3.

carbonyl groups from a bioctahedral $Fe_2(CO)_8$ structure and by taking proper, symmetry-adapted linear combinations of the four localized orbitals pointing to the missing carbonyls. Either way leads to the picture which is represented on the left side of Figure 2. Note, however, that we reoriented the sawhorse $Fe_2(CO)_6$ fragment of Figure 2 within the coordinate system as indicated in **I**. Different from **H**, this orientation and the concomitant location of two vicinal pairs of CO ligands within the *yz* and *xy* planes, respectively, seem more appropriate for the doubly bridged C_s arrangement of **A** and of complexes **5**, because this way the Fe_2S three-membered ring and the Fe_2C_3 substructure—orthogonal to each other—will also come to lie within these planes. Nevertheless, in order to retain consistency with the original electronic structure description for $M_2(CO)_6$ sawhorse fragments,[9] we will use the symmetry labels based upon **H** to characterize the MOs of $Fe_2(CO)_6$.

Figure 2 represents an interaction diagram, which constructs the MOs of a C_s $Fe_2(CO)_6(\mu\text{-}SH)^-$, the intended final bonding partner of the $C_3H_3^+$ bridge of **A**, from its constituent simpler fragments $Fe_2(CO)_6$ and SH^-. The bimetallic moiety is characterized by a low-lying nest of six orbitals of predominant d character (not labeled in Figure 2) which are derived from the t_{2g}-type MOs of two $Fe(CO)_3$ components. They are mostly involved in back-bonding to the six carbonyls and, apart from changing their relative ordering, are retained in Fe_2-

(10) Jemmis, E. D.; Hoffmann, R. *J. Am. Chem. Soc.* **1980**, *102*, 2570 and supplementary material.

(11) (a) Dickson, R. S.; Johnson, S. H.; Kirsch, H. P.; Lloyd, D. J. *Acta Crystallogr., Sect. B* **1977**, *33*, 2057. (b) Visser, J. P.; Schipperjin, A. J.; Lukas, J.; Bright, D.; de Boer, J. J. *Chem. Commun.* **1966**, 1266.

$(CO)_6(\mu\text{-SH})^-$. Of relevance with respect to the bonding of further ligands (e.g., of SH^-) to the $Fe_2(CO)_6$ fragment are those five valence orbitals at higher energy ($1a_1$ to $2a_1$), which are sketched in a qualitative way in Figure 2. When the SH^- group interacts with $Fe_2(CO)_6$ to form $Fe_2(CO)_6(\mu\text{-SH})^-$, two of these five valence MOs are utilized to make two Fe–S bonds and we are left with three valence orbitals (1a′, 2a′, and a″) for $Fe_2(CO)_6(\mu\text{-SH})^-$. Their shapes and energies are the result of interacting all lone-pair levels of SH^- shown in **B** and on the right side of Figure 2 with those of appropriate symmetry within the $1a_1$ to $2a_1$ frontier MO set of $Fe_2(CO)_6$. Because only C_s symmetry is retained for $Fe_2(CO)_6(\mu\text{-SH})^-$, these interactions between the two fragments lead to strong mixing of former $Fe_2(CO)_6$ levels ($1a_1$ with $1b_1$ and $2a_1$; $1a_2$ with $1b_2$), rehybridizing the two highest lying orbitals 2a′ and a″ of $Fe_2(CO)_6(\mu\text{-SH})^-$ as indicated in Figure 2. In a somewhat simplified manner they can be viewed as the symmetric and antisymmetric linear combination of two localized σ-type hybrids pointing to the two empty coordination sites of $Fe_2(CO)_6(\mu\text{-SH})^-$. Contour plots of a″ and 2a′, showing their true composition, and of the Fe–Fe σ-bonding orbital 1a′ (all MOs plotted within the *xz* plane of **I**) are given in Figure 3a. For a d^8–d^8 electron count these three frontier orbitals hold four electrons and the lower lying d-block of six levels is filled.

Also shown in Figure 3b are contour plots for those two orbitals (a_1 and b_2) of a ring-opened $C_3H_3^+$ ligand, which are derived from the broken C–C bond.[10] These two MOs, practically of identical energy for the specific geometry we have chosen here, are ideally prepared to overlap with 2a′ and a″ of $Fe_2(CO)_6(\mu\text{-SH})^-$, and we now are in a position to construct our model **A** by interacting the $Fe_2(CO)_6(\mu\text{-SH})^-$ unit with a C_3H_3 bridge. This is done in Figure 4, where all relevant MOs of the $C_3H_3^+$ ligand are displayed on the right side. The labels refer to C_{2v} symmetry. In addition to the two σ-overlapping orbitals a_1 and b_2 there are two π orbitals; the lower one (b_1) is filled, and the upper one (a_2) is an acceptor level ready for back-bonding. The third π MO of the organic ligand is much too high in energy to interact significantly with the metal fragment and is therefore not shown in Figure 4. The attachment of an additional ligand again causes extensive mixing within the six d-block orbitals of the $Fe_2(CO)_6(\mu\text{-SH})^-$ fragment. As expected, however, the essential bonding interactions between $Fe_2(CO)_6(\mu\text{-SH})^-$ and $C_3H_3^+$ occur between both pairs of σ-overlapping frontier MOs (2a′, a″ and a_1, b_2, respectively) and two Fe–C σ bond are formed. The energy of the Fe–Fe σ-bonding MO 1a′ of $Fe_2(CO)_6(\mu\text{-SH})^-$ is nearly unaffected because it is part of a typical three-orbital pattern. It is destabilized by a_1 of $C_3H_3^+$, but simultaneously it is kept at low energy by mixing into itself the 2a′ metal level from above. As one goes from $Fe_2(CO)_6(\mu\text{-SH})^-$ to the complete molecule $Fe_2(CO)_6(\mu\text{-SH})(\mu\text{-}C_3H_3)$ the Fe–Fe σ-bonding orbital becomes the HOMO a′. The LUMO a″ of the complex evolves from the unfilled, antisymmetric π orbital a_2 of $C_3H_3^+$, which interacts with a filled MO of appropriate symmetry within the d block of $Fe_2(CO)_6(\mu\text{-SH})^-$. In the complex, this interaction transfers a total of 0.316 electron into the formerly empty a_2 orbital of the C_3H_3 unit. The HOMO–LUMO gap of our unsubstituted model complex is rather small and amounts to approximately 1 eV. There is no fully delocalized π system in the Fe_2C_3 five-membered ring because the π interactions Fe–Fe, Fe–C, and C–C involve energetically very different d- and p-type basis functions with widely differing overlaps. A description of such systems in terms of "aromatic" or "nonaromatic" character[8c] therefore does not seem to be too meaningful. We rather have to describe $Fe_2(CO)_6(\mu\text{-SH})(\mu\text{-}C_3H_3)$ as being composed of an ideally delocalized C_3 bridge, coupled to the diiron moiety by two strong σ bonds and by moderate π back-bonding. The two resonance structures presented earlier in this paper certainly are a proper description for compounds **5**. They also indicate that, apart from the metal–metal bond, the electronic structure of the dinuclear compounds **5** and of their model **A** bears some similarity to mononuclear "Fisher-type" carbene complexes.[6a,7] There, a carbene-centered p-type MO is the LUMO, and this in a sense is just half of the LUMO shown in Figure 3 and in ref 8c.

At this point we should recall that our model system **A** has not only been simplified by replacing the real S and C substituents by hydrogens; so far we have also kept an idealized sawhorse geometry (**H**, **I**) for the $Fe_2(CO)_6$ fragment in both $Fe_2(CO)_6(\mu\text{-SH})^-$ and $Fe_2(CO)_6(\mu\text{-SH})(\mu\text{-}C_3H_3)$. The actual structure of **5a** shows some interesting distortions, which may be conveniently and quite accurately described by simple angular motions of the CO groups as given in **J**. Compared with our

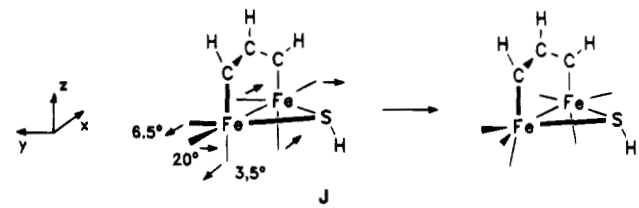

model, the two CO groups which are colinear with the Fe–Fe vector in **A** move within the *xy* plane and bend toward the sulfur bridge by ca. 20°. The two carbonyl ligands *trans* to μ-S follow this motion by 6.5°, and the two CO ligands *trans* to the μ-C_3 carbons bend away from the Fe–Fe bond, roughly within the *xz* plane. In addition, the interplanar angle between the two ring planes of Fe_2C_3 and Fe_2S is not 90° as in **A** but is opened up to 99°. When we abandon our geometric restrictions and allow these angular variables to relax simultaneously (all Fe–C–O kept linear), the lowest energy is indeed found for precisely the CO ligand arrangement as in **J**. Instead of 99° the Fe_2C_3 and Fe_2S planes form an angle of 92°, but this 7° difference may be due to our replacement of the bulky μ-S-*t*-Bu by μ-SH.

The basic electronic structure discussed above, of course, remains qualitatively unchanged by these molecular distortions, which altogether only lead to a lowering of the total energy by some 13 kcal compared to the idealized geometry **A** and which serve to improve the overlap situation and to diminish intramolecular repulsions.[12] We have also varied the pyramidality at the sulfur atom, allowing the S–H bond to swing from an *exo* (as in **A** and **5**) to an *endo* position, passing through a trigonal-planar arrangement around S. The lower energy is calculated for SH pointing to the *exo* direction, as found for *t*-BuS in the real system. For steric reasons the pyramidality at sulfur is less pronounced in **5a** than in its model: the S–H vector is bent

(12) Teo, B. K.; Hall, M. B.; Fenske, R. F.; Dahl, L. F. *Inorg. Chem.* **1975**, *14*, 3103.

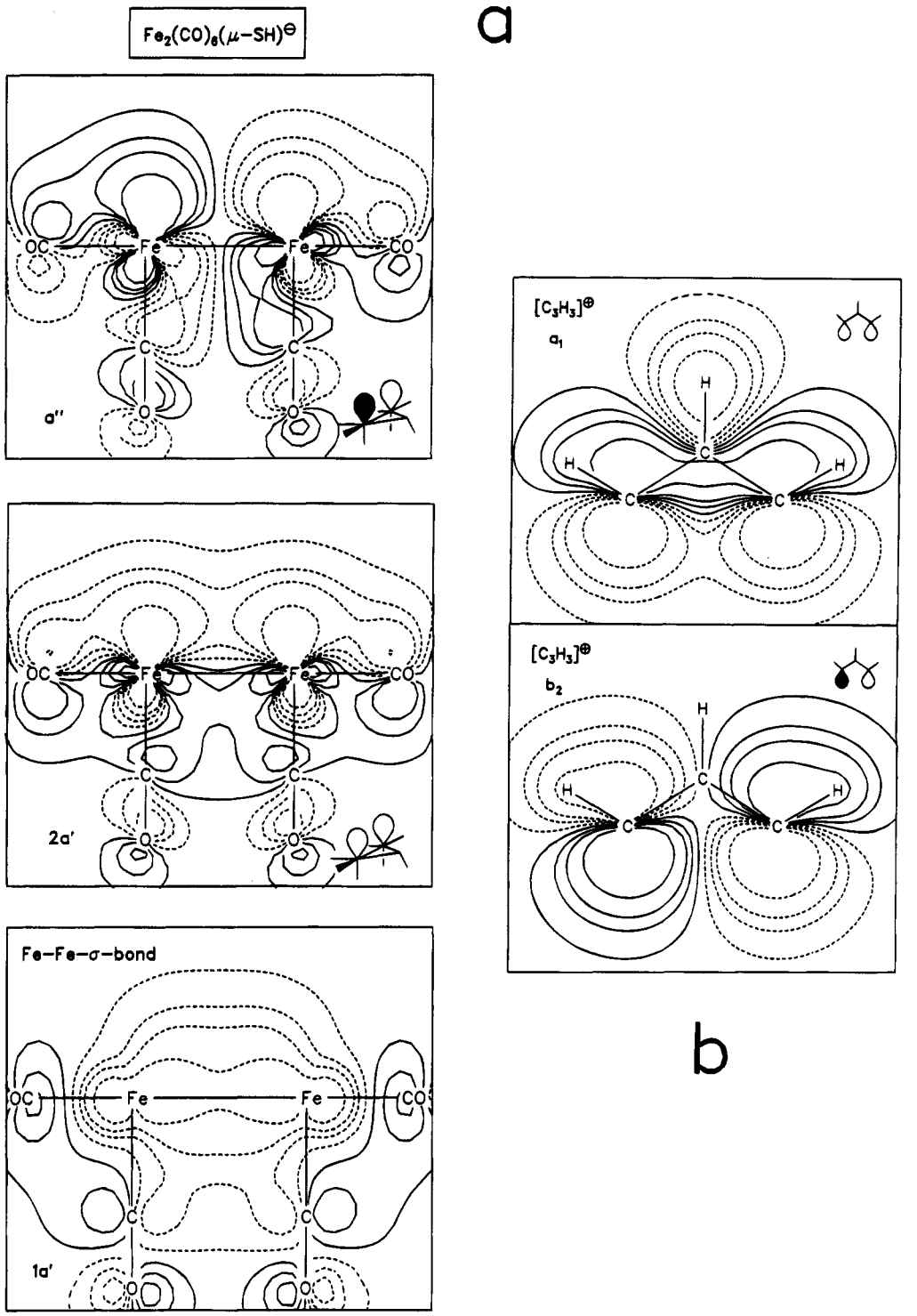

Figure 3. (a) Contour maps of the three valence MOs a″, 2a′, and 1a′ of $Fe_2(CO)_6(\mu\text{-}SH)^-$. (b) Contour maps of the two frontier MOs a_1 and b_2 of the ring-opened $C_3H_3^+$ fragment, plotted in the molecular plane. The contour levels of the wave functions are 0.1, 0.05, 0.03, and 0.01 in atomic units, with negative values given as dashed lines.

down out of the Fe_2S plane by 62° in **A**, whereas the corresponding S–C bond of **5a** makes an angle of only 51°. The inversion barrier at sulfur is only around 12 kcal, but the *endo* position is less favorable even for H. For a *t*-Bu substituent the *exo* orientation is mandatory for steric reasons anyway. We note in this context that for compounds **7**, where a smaller acyl group replaces the bridging C_3R_3 fragment, an *endo* isomer has been isolated even for μ-S-*t*-Bu as the other bridge (*vide infra*).

In reference back to Figure 4 and to the implied analogy of complexes **5** to "Fischer-type" carbene complexes, this similarity should have some further consequences. Typically, the kinetic and thermodynamic stability of such carbene complexes increases if the carbene carbon is substituted by π-donor groups such as NR_2, OR, OCOR, and the like. The bonds toward these substituents then usually display considerable C–N, C–O, etc. double-bond character. As already mentioned above, this is exactly what has been seen in the X-ray structure of **5a**. Quite obviously and directly analogous to the case of "Fischer carbenes",[6a] the LUMO will be pushed up and the small HOMO–LUMO gap of the unsubstituted parent molecule **A** should accordingly

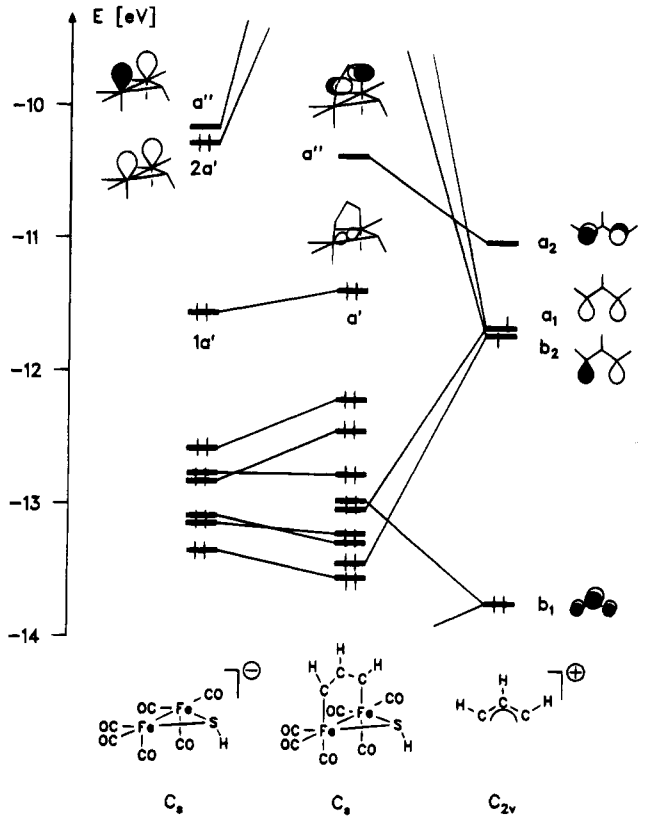

Figure 4. Orbital interaction diagram for $Fe_2(CO)_6(\mu\text{-SH})(\mu\text{-}C_3H_3)$ (**A**). For details see text.

become larger, if π-donor groups are connected to the two terminal carbons of the μ-C_3 bridge, which carry the main portion (80% for **A**) of the LUMO wave function. Substitution at the central carbon will have no great consequences. To be most efficient for π donation, the relative orientation of such donor groups with respect to the C_3 unit should optimize π overlap. The substitution pattern of compounds **5** and the orientation of OEt and $OC(O)CH_3$ groups in the crystal of **5a** nearly perfectly reflect these electronic requirements.

To check these conclusions, we have performed model calculations for a series of substituted derivatives of **A** as shown in **K**. For the monohydroxy compound (R^1 = OH, R^2 = H) the HOMO–LUMO gap has already increased to 1.47 eV. Replacing the second (terminal) hydrogen by OH or by O^- as well opens the frontier orbital gap to 1.91 eV, indicating "nonaromatic" character according to a recent classification by Chamizo and co-workers,[8c] or—as we would prefer to put it—securing a stable closed-shell ground state with moderate Fischer-type carbene reactivity due to the high energy of the LUMO. When we model the actual substitution pattern of compound **5a** by a formate and a hydroxy group (R^1 = HCOO, R^2 = OH), the gap is 1.75 eV. For all cases the energy fo the HOMO, representing the Fe–Fe bond, stays constant and the carbon-to-iron bonds

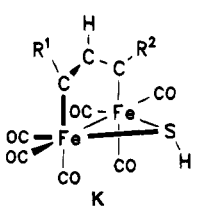

K

R^1 = OH, R^2 = H

R^1 = OH, R^2 = OH

R^1 = HCOO, R^2 = OH

R^1 = O^-, R^2 = OH

Table 2. ^{13}C and ^1H NMR Data for 5

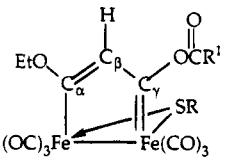

	$\delta(C_\alpha)$	$\delta(C_\beta)$	$\delta(C_\gamma)$	$\delta(H_\beta)$
5a	284.82	136.06 (d)	267.43	6.85
5b	284.14	136.16 (d)	267.15	6.99
5c	283.76	136.28 (d)	266.07	6.81

are not affected either. For R^1 = HC(O)O and R^2 = OH, the electronically slightly unsymmetric substitution pattern (acyloxy vs alkoxy) causes only a very small asymmetry within the C_3 bridge: the computed reduced overlap population of the C–C bond on the OH-substituted side is 1.110, while that toward the HC(O)O-carrying carbon is 1.125, indicating a stronger and thus shorter C–C bond from the central to the acetoxy-substituted carbon. The corresponding C–C distances observed for **5a**, 1.365(11) and 1.392(11) Å, show exactly this trend.

Summarizing the results of our model calculations, we think that compounds **5** can be viewed as a special class of dinuclear, "Fischer-type" iron bis(carbene) complexes, in which a delocalized C_3R_3 unit, equivalent to a ring-opened or bond-stretched cyclopropenium ligand, plays the role of the μ-bis(carbene) bridge and provides that appropriate LUMO. Different from the case for mononuclear carbene complexes, the metal–metal bond is the HOMO for these systems.

The ^{13}C NMR spectra of complexes **5** are in agreement with their formulation as carbene complexes. As shown in Table 2, the ^{13}C NMR signals of the bridging ligand carbon atoms bonded to Fe are around δ_C 284 (C_α) and δ_C 267 (C_γ), which is within the range for metal–carbene carbon atom signals.[13] The ^{13}C NMR signal of C_β is in the olefinic region,[14] as is the ^1H resonance of its attached proton.[15] The IR spectra all showed a strong carbonyl absorption (ca. 1748–1780 cm^{-1}), which can be assigned to the ester moiety derived from *acylation* of the *oxygen*-centered anion **6**.[16] The methyl resonances of the *tert*-butyl group in the ^1H and ^{13}C NMR spectra of **5a,b** (δ_H ~1.4 and δ_C ~34.0) indicate that the thiolate group bridges the two iron atoms and therefore does not interact with the vinylcarbene bridge.[1,2,3d,e]

A possible mechanism of formation of **5a–c** is outlined in Scheme 1. Initially, attack by the iron-centered $[(\mu\text{-CO})(\mu\text{-RS})Fe_2(CO)_6]^-$ anion at the α-carbon atom of EtOC≡CH leads to the formation of a β-vinylic anion (Li^+ cation). This carbanionic site is in close proximity to both bridging and terminal CO ligands within the molecule, and intramolecular attack by the carbanion at the carbon atom of a CO ligand follows. This is the intramolecular analog of the intermolecular attack of an organolithium reagent on a mononuclear metal carbonyl, the first step in the synthesis of Fischer-type carbenes.[17] In the present case, a stable, electron-rich, and resonance-stabilized anionic Fischer-type oxycar-

(13) Mann, B. E.; Taylor, B. F. *^{13}C NMR Data for Organometallic Compounds*; Academic Press: New York, 1981; p 172.
(14) *Interpretation of Carbon-13 NMR Spectra*; Wehrli, F. W.; Wirthlin, T., Eds.; Wiley: New York, 1983; p 311.
(15) *Spectrometric Identification of Organic Compounds*; Silverstein, R. M., Bassler, G. C., Morrill, T. C., Eds.; Wiley: New York, 1981.
(16) Reference 15, pp 108, 117.

Scheme 1

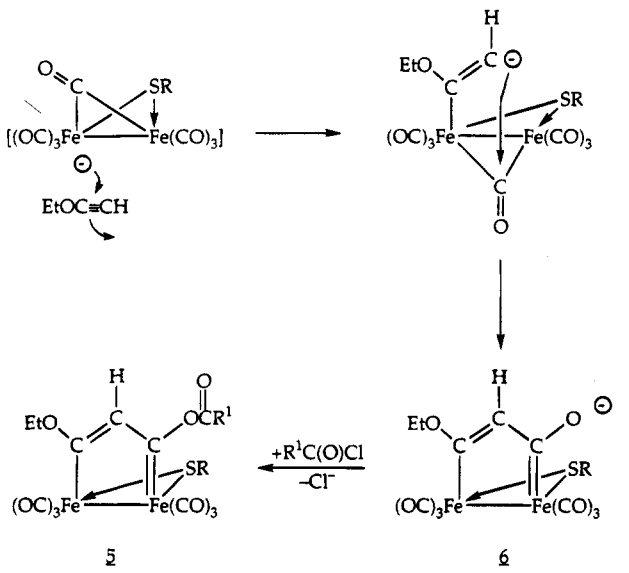

Table 3. ^{13}C and ^{1}H NMR Data for 6

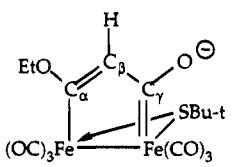

$\delta(C_\alpha)$	$\delta(C_\beta)$	$\delta(C_\gamma)$	$\delta(H_\beta)$
259.78	125.52	231.63	5.27

bene species, **6**, is generated. Its acylation by RC(O)Cl at oxygen then gives the observed product, **5**.

In an effort to provide experimental proof for this suggested mechanism, we have isolated what we believe to be the anionic intermediate, **6** (R = *t*-Bu), from the crude reaction mixture as the Li^+/12-crown-4-salt. In comparison to the neutral complexes (μ-EtOC=C(H)C-(OC(O)R³)=)(μ-RS)$Fe_2(CO)_6$ (**5**), the IR spectrum of **6** shows the terminal carbonyl absorptions shifted somewhat to a lower wavenumber, which is consistent with an increase of electron density on the iron centers. This phenomenon is likewise evident in the ^{13}C NMR spectrum, where the terminal carbonyl resonances are shifted slightly downfield as compared to those observed in the ^{13}C NMR spectrum of **5**. For the same reason, the carbon-13 NMR resonances of the vinylcarbene bridge are conversely shifted *upfield* (compare Tables 2 and 3). As expected, the greatest effect is observed for C_γ, the carbene atom adjacent to the negatively charged oxygen atom, which is shifted approximately 35 ppm upfield (δ_C ~267 in **5** vs 231.6 in **6**). Due to this increase of electron density in the ring ligand, C_α and C_β are similarly shifted upfield relative to **5** by approximately 24 and 11 ppm, respectively. (An upfield shift is likewise observed for the proton attached to C_β in the corresponding ^{1}H NMR spectrum.) Finally, delocalization of electron density onto the thiolate bridge is observed in the upfield shift of the ipso *tert*-butyl carbon atom resonance from ~50 ppm in **5a,b** to 34.57 ppm in **6**.

Attempted interception of anion **6** by protonation rather than acylation led to unexpected results. Addition of an equimolar amount of neat trifluoroacetic acid at room temperature to the Li[(μ-CO)(μ-RS)$Fe_2(CO)_6$]/ethoxyacetylene reaction mixture (with stirring for 30 min) did not yield stable hydroxyvinylcarbene analogs of **5**, but instead, the α,β-unsaturated bridging acyl species (μ-EtOC(=CH_2)C=O)(μ-RS)$Fe_2(CO)_6$ (**7**) were formed in good yield (eq 4). While hydroxyvinylcarbene

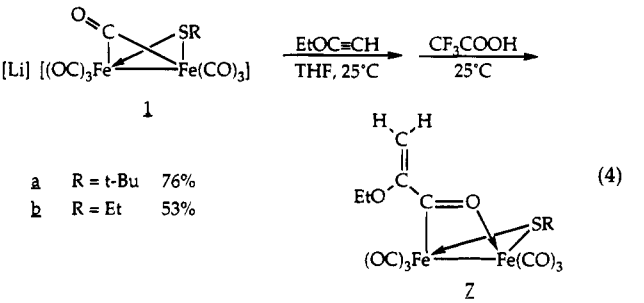

(4)

species may be the initially formed intermediates, a complex, secondary rearrangement must occur which ultimately yields the new bridging acyl products (eq 5).

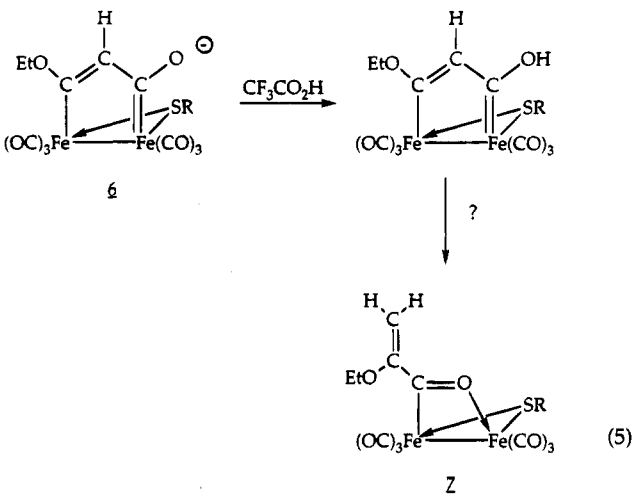

(5)

These μ-acyl complexes, like some others of this class,[18] are unstable toward decarbonylation, readily losing CO to give the vinyl species (μ-η¹:η²-EtOC=CH_2)(μ-RS)Fe_2-$(CO)_6$ (**8**) in nearly quantitative yield at room temperature in THF (eq 6). In order to confirm the structure of

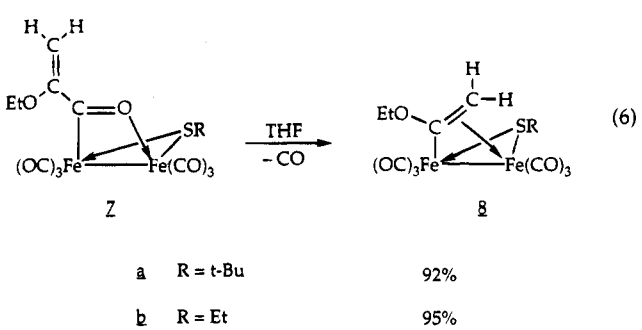

(6)

7, a single-crystal X-ray diffraction study of **7a** was undertaken. An ORTEP plot showing 30% probability thermal ellipsoids and the atom-labeling scheme is shown in Figure 5. Pertinent bond distances and angles are shown in Table 4. Here also, a carbonyl ligand has been incorporated into the organic framework, but the structure is quite different. The acetylenic portion of

(17) Fischer, H. In *Transition Metal Carbene Complexes*; Dötz, K. H., Fischer, H., Hofmann, P., Kreissl, F. R.; Schubert, U., Weiss, K., Eds.; Verlag Chemie: Weinheim, Germany, 1983; pp 1–68.

(18) Seyferth, D.; Archer, C. M.; Ruschke, D. P.; Cowie, M.; Hilts, R. W. *Organometallics* **1991**, *10*, 3363.

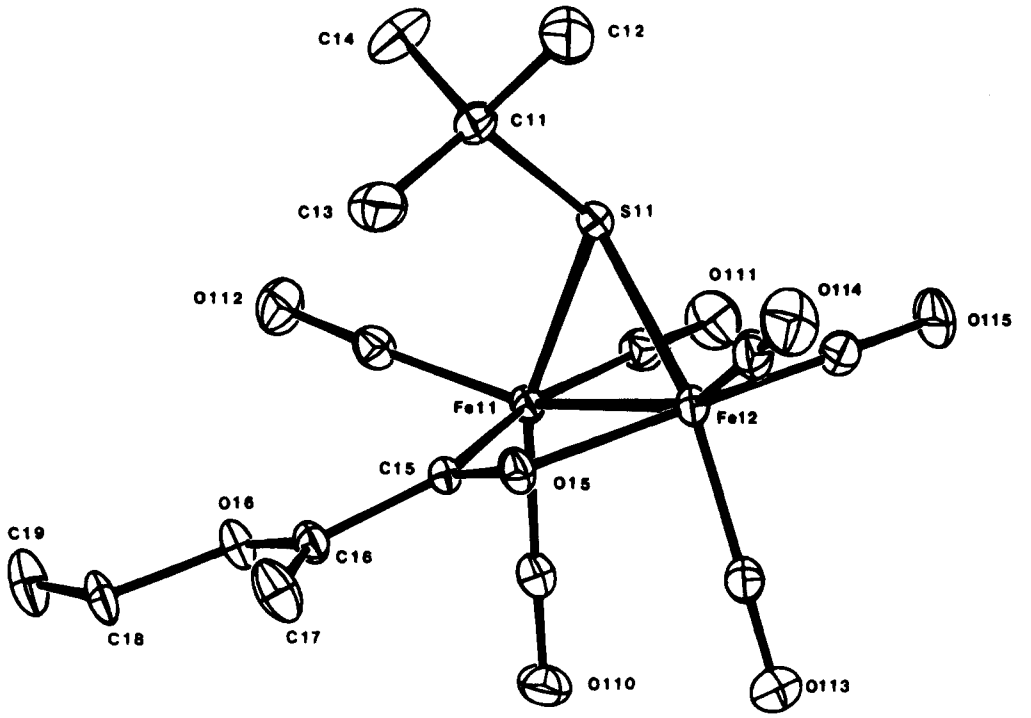

Figure 5. ORTEP diagram of **7a** showing 30% probability thermal ellipsoids.

Table 4. Relevant Bond Distances (Å) and Angles (deg) for 7a

Fe(11)–Fe(12)	2.565(1)	C(18)–C(19)	1.518(6)
Fe(11)–C(15)	1.930(3)	Fe(11)–S(11)	2.253(1)
Fe(11)–O(15)	2.704	Fe(12)–S(11)	2.243(1)
Fe(12)–O(15)	1.976(2)	S(11)–C(11)	1.865(4)
Fe(12)–C(15)	2.586(3)	C(11)–CH_3 (mean)	1.532
C(15)–O(15)	1.248(4)	Fe(11)–CO (mean)	1.806
C(15)–C(16)	1.504(4)	Fe(11)C–O (mean)	1.143
C(16)–C(17)	1.337(5)	Fe(12)–CO (mean)	1.803
C(16)–O(16)	1.351(4)	Fe(12)C–O (mean)	1.137
O(16)–C(18)	1.449(4)		
Fe(11)–Fe(12)–O(15)	71.8(1)	O(16)–C(18)–C(19)	108.0(3)
Fe(12)–Fe(11)–C(15)	68.6(1)	C(16)–O(16)–C(18)	115.3(3)
Fe(11)–C(15)–O(15)	115.0(2)	Fe(11)–S(11)–Fe(12)	69.6(0)
Fe(11)–C(15)–C(16)	130.2(3)	Fe(12)–Fe(11)–S	55.0(0)
Fe(12)–O(15)–C(15)	104.4(2)	Fe(11)–Fe(12)–S	55.4(0)
C(15)–C(16)–C(17)	120.4(3)	O(15)–Fe(12)–S(11)	90.2(1)
C(15)–C(16)–O(16)	112.6(3)	C(15)–Fe(11)–S(11)	90.2(1)
O(15)–C(15)–C(16)	114.7(3)	Fe(11)–S(11)–C(11)	120.9(1)
O(16)–C(16)–C(17)	127.0(3)	Fe(12)–S(11)–C(11)	119.7(1)

the ligand is no longer bound to iron as in **5** but is attached by the α-carbon atom to the acyl bridge which is derived from a CO ligand. Protonation at the β-carbon atom of the acetylenic moiety then gives rise to the pendant vinyl substituent. These μ-α,β-unsaturated acyl products were isolated as inseparable mixtures of two isomers, presumably resulting from either an axial (a) or equatorial (e) orientation of the organic group on the sulfur atom of the symmetrical thiolate bridge (Figure 6). The crystal isolated for the X-ray crystallographic study was the axial isomer of **7a**.

Surprisingly, the X-ray structure of **7a** shows little electron delocalization over the vinyl portion of the acyl bridge. The C(15)–C(16) bond length of 1.504(4) Å is typical for carbon–carbon single bonds adjacent to a carbonyl unit (1.516(5) Å),[4] and the C(16)–C(17) bond of 1.337(4) Å shows no lengthening from that of a typical carbon–carbon double bond (1.337(6) Å).[4] The C(16)–O(16) distance of 1.351(4) Å does show some shortening from that of a simple carbon–oxygen single bond (1.43(1) Å),[4] but remarkably, the C(18)–O(16) bond

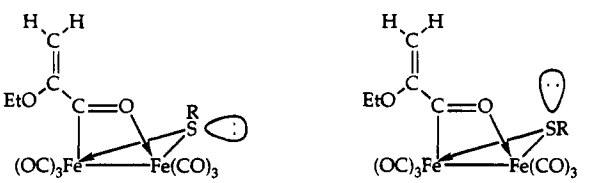

Figure 6. Axial (a) and equatorial (e) isomers of (μ-EtOC(=CH_2)C=O)(μ-RS)$Fe_2(CO)_6$.

of 1.449(4) Å remains largely unaffected. In contrast to these findings, Carty and his co-workers have reported the crystal structure of a related complex, (μ-HC(=C(Ph)NHPh)C=O)(μ-Ph_2P)$Fe_2(CO)_6$, which was found to have considerable electron delocalization over the entire α,β-unsaturated acyl bridge.[19] As expected, however, electron delocalization in the bridging acyl frament of **7a** is indicated. The C(15)–O(15) distance of 1.248(4) Å is longer than that of a typical conjugated, carbon–oxygen double bond,[4] although it is somewhat shorter than those in related acyl-bridged complexes.[6,19,20] Conversly, the short Fe(11)–C(15) bond of 1.930(3) Å is consistent with known μ-acyl or related "carbene-like" ligands (i.e., μ-thioacyl, μ-vinyl, μ-acetylide).[5,19,21]

Once the structure of these new α,β-unsaturated acyl species was determined with certainty, the analytical and spectroscopic data obtained for **7** were readily understandable. In general, a very strong band at 1480 cm^{-1} in the infrared spectra of these complexes can be assigned to the carbonyl absorptions of the bridging acyl ligands.[18,22] The presence of the uncomplexed C=C bond of the vinyl portion of the ligand is indicated by a

(19) Mott, G. N.; Granby, R.; MacLaughlin, S. A.; Taylor, N. J.; Carty, A. J. *Organometallics* **1983**, *2*, 189.
(20) (a) Yu, Y.-F.; Gallucci, J.; Wojcicki, A. *J. Am. Chem. Soc.* **1983**, *105*, 4826. (b) Rosen, R. P.; Hoke, J. B.; Whittle, R. R.; Geoffroy, G. L.; Hutchinson, J. P.; Zubieta, J. A. *Organometallics* **1984**, *3*, 846.
(21) Patin, H.; Mignani, G.; Benoit, A.; Le Marouille, J.-Y.; Grandjean, D. *Inorg. Chem.* **1981**, *20*, 4351.
(22) Seyferth, D.; Womack, G. B.; Dewan, J. C. *Organometallics* **1985**, *4*, 398.

medium band at 1600 cm^{-1} in the IR spectrum,[16] as well as in the ^1H and ^{13}C NMR spectra by appropriate vinyl resonances. In the ^{13}C NMR spectra, the acyl moiety gives rise to a pair of singlets (two isomers!) far downfield (σ_C ~285 ppm) in the region typically reported for related acyl- and thioacyl-bridged clusters.[20-22] Although **7a** could be isolated as a red, crystalline solid, **7b** was isolated as a slightly air sensitive, red oil which, when coupled with its tendency to undergo decarbonylation, could not be purified sufficiently to give an accurate C/H combustion analysis.

Certainly, the chemistry of the Li[(μ-CO)(μ-RS)Fe_2-$(CO)_6$]/ethoxyacetylene system is dominated by complex rearrangement mechanisms operating at room temperature. As with the reactions of this salt with the electrophilic acetylenes dimethylacetylenedicarboxylate, methyl propiolate, and 3-butyn-2-one,[2] these intramolecular rearrangements resulting in carbon monoxide incorporation are disfavored at low temperature. For instance, reaction of Li[(μ-CO)(μ-*t*-BuS)$Fe_2(CO)_6$] with ethoxyacetylene at −78 °C followed by reaction of the anionic intermediate with trifluoroacetic acid at −78 °C gave (μ-EtOC(=CH_2)C=O)(μ-*t*-BuS)$Fe_2(CO)_6$ (**7a**) in only 17% yield with the major product being (μ-η^1:η^2-EtOC=CH_2)(μ-*t*-BuS)$Fe_2(CO)_6$ (**8a**) in 58% yield (eq 7).

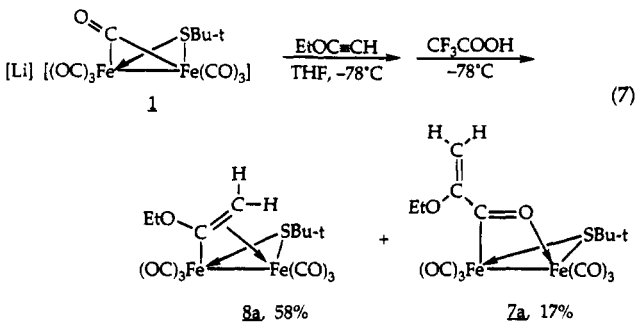

(7)

It may be that the initial intermediate **9** is sufficiently long-lived at −78 °C (with respect to the intramolecular process shown in Scheme 1) that it can be protonated at carbon, giving ultimately, with loss of CO, the μ-η^1:η^2-vinyl compound **8**. This compound (R = *t*-Bu) also was prepared in high yield by the reaction of [Et_3NH]-[μ-CO)(μ-*t*-BuS)$Fe_2(CO)_6$] with ethoxyacetylene at room temperature.[1]

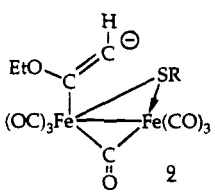

Experimental Section

General Comments. All reactions were carried out under an atmosphere of prepurified tank nitrogen. Tetrahydrofuran (THF) was distilled under nitrogen from sodium/benzophenone ketyl and purged with nitrogen prior to use. Triethylamine was distilled under nitrogen from calcium hydride and purged with nitrogen prior to use. Ethyl, *tert*-butyl, phenyl, and benzyl mercaptans were purged with nitrogen and used without further purification. Acetyl, benzoyl, and pivaloyl chlorides were all freshly distilled and purged with ntirogen prior to use. 12-Crown-4 (Aldrich) was purged with nitrogen and used without further purification. Trifluoroacetic acid was purified by vacuum distillation (at room temperature) and purged with nitrogen prior to use. Ethoxyacetylene (purchased from Farchan Laboratories) was purged with nitrogen after purification by vacuum distillation (at room temperature) when necessary. Triiron dodecacarbonyl was prepared by a literature procedure,[23] and *n*-butyllithium (2.4 M in hexane) was purchased from Alfa and used as received.

Table 5. Crystal Data for (μ-EtOC=CHC(OC(O)Me)=)(μ-*t*-BuS)$Fe_2(CO)_6$ (5a)

a = 9.583(2) Å	β = 93.37(1)°
b = 14.176(3) Å	ϱ(calcd) = 1.541 g cm^{-3}
c = 16.206(2) Å	μ = 14.2 cm^{-1} [a]
V = 2197.8 $Å^3$	Z = 4
Space group: $P2_1/n$	

[a] A semiempirical absorption correction was applied.

The progress of all reactions was monitored by thin-layer chromatography (Baker-Flex Silica Gel, 1B-F). Purification by filtration chromatography in which the reaction products were dissolved in a suitable solvent and chromatographed on a bed of EM Science or Sigma 100−300-mesh silicic acid (ca. 200 mL) in a 350-mL glass fritted filter funnel was used in most cases. Further purification by medium-pressure column chromatography was accomplished with a 300 × 25 mm or a 450 × 25 mm column using Sigma 230−400-mesh silica gel. All chromatography was completed without exclusion of atmospheric moisture or oxygen. Solid products were recrystallized from deoxygenated solvents at −20 °C.

Solution infrared spectra (NaCl windows) were obtained using a Perkin-Elmer Model 1430 double-beam grating infrared spectrophotometer. Proton NMR spectra were recorded on a JEOL FX-90Q, a Bruker WM-250, or a Varian XL-300 NMR spectrometer operating at 90, 250, or 300 MHz, respectively. Carbon-13 NMR spectra were obtained using a Bruker WH-270 or Varian XL-300 spectrometer operating at 67.9 or 75.4 MHz, respectively. Electron impact mass spectra were obtained using a Finnigan 3200 mass spectrometer operating at 70 eV. Field desorption mass spectra were obtained with a Finnigan MAT-731 mass spectrometer operating in the positive ion mode. FAB mass spectra were obtained with a Finnigan MAT-731 mass spectrometer operating in the negative ion mode. All masses were correlated using the following isotopes: ^1H, ^7Li, ^{12}C, ^{16}O, ^{32}S, and ^{56}Fe. Melting points were determined in air on a Büchi melting point apparatus using analytically pure samples and are uncorrected. Microanalyses were performed by Scandinavian Microanalytical Laboratory, Herlev, Denmark.

X-ray Crystallography.[24] **(μ-EtOC=C(H)C(OC(O)Me)=)-(μ-*t*-BuS)$Fe_2(CO)_6$ (5a).** Data in the range 3° ≤ 2θ ≤ 55° were collected using Mo Kα radiation on an Enraf-Nonius CAD4F-11 diffractometer. Data collection, reduction, and refinement procedures have been detailed elsewhere.[25] Hydrogen atoms were ignored, while all other atoms were refined anisotropically. Final R_1 = 0.069 and R_2 = 0.073 for 2360 observed reflections ($+h,+k,\pm l$; $I_o > 2\sigma(I_o)$) and 262 variables. The largest peak on the difference-Fourier map was 0.68 e $Å^{-3}$. Crystal data are summarized in Table 5, and final positional parameters appear in Table 6.

(μ-EtOC(=CH_2)C=O)(μ-*t*-BuS)$Fe_2(CO)_6$ (7a). Data in the range 3° ≤ 2θ ≤ 55° were collected at −65 °C using MoKα radiation on an Enraf-Nonius CAD4F-11 diffractometer equipped with a liquid-nitrogen low-temperature device. Data collection, reduction, and refinement procedures have been detailed elsewhere.[25] Hydrogen atoms were ignored, while all other atoms were refined anisotropically. Final R_1 = 0.044 and R_2 = 0.060 for 3769 observed reflections ($\pm h,\pm k,+l$; $I_o > 2\sigma(I_o)$) and 235 variables. The largest peak on the difference-Fourier map was 0.69 e $Å^{-3}$. The structure solution proved difficult and was initially obtained in space group $P1$ and then

(23) McFarlane, W.; Wilkinson, G. *Inorg. Synth.* **1966**, *8*, 181.
(24) These structures were reported in our preliminary communication, and the supplementary material was deposited with this paper: Hoke, J. B.; Dewan, J. C.; Seyferth, D. *Organometallics* **1987**, *6*, 1816.
(25) Silverman, L. D.; Dewan, J. C.; Giandomenico, C. M.; Lippard, S. J. *Inorg. Chem.* **1980**, *19*, 3379.

Table 6. Final Positional Parameters for 5a

atom	x	y	z
Fe(1)	−0.01635(12)	0.25952(8)	−0.10122(7)
Fe(2)	0.03455(13)	0.26530(9)	0.05980(7)
S	0.1649(2)	0.18949(15)	−0.03083(14)
C(11)	−0.1821(10)	0.3143(6)	−0.1003(6)
O(11)	−0.2895(7)	0.3479(5)	−0.0986(5)
C(12)	−0.0078(10)	0.2308(6)	−0.2075(6)
O(12)	−0.0045(9)	0.2171(5)	−0.2765(4)
C(13)	0.0656(10)	0.3709(7)	−0.1198(6)
O(13)	0.1111(8)	0.4427(5)	−0.1366(5)
C(21)	−0.1284(11)	0.3128(7)	0.0861(6)
O(21)	−0.2328(8)	0.3394(6)	0.1041(5)
C(22)	0.1227(11)	0.2447(7)	0.1578(7)
O(22)	0.1759(9)	0.2309(6)	0.2221(5)
C(23)	0.1057(11)	0.3832(7)	0.0552(6)
O(23)	0.1403(9)	0.4596(5)	0.0572(5)
C(31)	0.3485(9)	0.2280(7)	−0.0471(6)
C(32)	0.4411(11)	0.1555(9)	0.0060(8)
C(33)	0.3830(10)	0.3309(7)	−0.0162(7)
C(34)	0.3676(12)	0.2209(9)	−0.1396(7)
C(41)	−0.3445(14)	0.0023(8)	−0.2226(7)
C(42)	−0.2791(12)	0.0209(7)	−0.1368(6)
O(41)	−0.1840(7)	0.1037(4)	−0.1466(4)
C(43)	−0.1173(9)	0.1410(6)	−0.0810(5)
C(44)	−0.1251(9)	0.0964(6)	−0.0049(5)
C(45)	−0.0621(9)	0.1429(6)	0.0610(5)
O(42)	−0.0590(7)	0.1007(5)	0.1366(4)
C(46)	−0.1601(15)	0.0549(10)	0.1713(9)
O(43)	−0.2801(12)	0.0615(8)	0.1419(7)
C(47)	−0.1190(14)	0.0061(8)	0.2495(7)

Table 7. Crystal Data for (μ-EtOC(=CH_2)C=O)(μ-*t*-BuS)$Fe_2(CO)_6$ (7a)

$a = 11.125(3)$ Å	$\alpha = 100.88(2)°$
$b = 11.400(2)$ Å	$\beta = 91.57(2)°$
$c = 7.820(3)$ Å	$\gamma = 85.37(2)°$
$V = 970.7$ Å^3	$\mu = 16.0$ cm^{-1} [a]
$Z = 2$	ϱ(calcd) = 1.601 g cm^{-3}
space group: $P\bar{1}$	

[a] A semiempirical absorption correction was applied.

Table 8. Final Positional Parameters for 7a

atom	x	y	z
Fe(11)	0.21557(4)	0.29484(4)	0.19319(6)
Fe(12)	0.12703(4)	0.23214(4)	0.45879(6)
S(11)	0.16614(7)	0.10862(7)	0.20394(11)
O(15)	0.3016(2)	0.2468(2)	0.5015(3)
O(16)	0.4969(2)	0.3618(2)	0.2453(3)
O(110)	0.2109(3)	0.5546(2)	0.3104(4)
O(111)	−0.0101(3)	0.3230(3)	−0.0131(4)
O(112)	0.3810(3)	0.2482(3)	−0.1033(4)
O(113)	0.0856(3)	0.4716(3)	0.6767(4)
O(114)	0.1059(3)	0.0691(3)	0.7083(5)
O(115)	−0.1259(2)	0.2317(3)	0.3501(5)
C(11)	0.2845(3)	−0.0180(3)	0.1938(5)
C(12)	0.2201(5)	−0.1162(4)	0.2566(8)
C(13)	0.3997(4)	0.0104(4)	0.3003(8)
C(14)	0.3137(5)	−0.0558(4)	0.0005(6)
C(15)	0.3362(3)	0.2847(3)	0.3729(4)
C(16)	0.4634(3)	0.3217(3)	0.3874(5)
C(17)	0.5303(4)	0.3131(5)	0.5298(6)
C(18)	0.6215(3)	0.3904(4)	0.2453(6)
C(19)	0.6456(4)	0.4240(5)	0.0712(7)
C(110)	0.2135(3)	0.4531(3)	0.2627(5)
C(111)	0.0767(3)	0.3101(3)	0.0647(5)
C(112)	0.3182(3)	0.2689(3)	0.0135(5)
C(113)	0.1010(3)	0.3786(4)	0.5931(5)
C(114)	0.1139(3)	0.1319(4)	0.6140(5)
C(115)	−0.0269(3)	0.2325(3)	0.3931(5)

transformed to $P\bar{1}$. Crystal data are summarized in Table 7, and final positional parameters are given in Table 8.

MO Calculations. The MO calculations were of the extended Hückel type.[8a,b] Atomic parameters for C, O, and H are standard ones;[8a,b] those for S[26] and Fe[27] have been taken from earlier work. A modified Wolfsberg–Helmholz formula[28] for calculating the off-diagonal matrix elements H_{ij} was used throughout. The molecular geometries were adapted from the X-ray structure of **5a** and idealized within C_s symmetry. Unless stated otherwise in the text or varied within geometry optimizations, the following geometric parameters were used for **A** or its component molecular fragments. Distance(s): Fe–Fe = 2.638 Å, Fe–S = 2.256 Å, Fe–CO = 1.78 Å, C–O = 1.14 Å, S–H = 1.33 Å, Fe–C_{C3} = 1.97 Å, C–C = 1.38 Å, C–H = 1.08 Å, O–H = 1.00 Å, C–O_{HCOO} = 1.32 Å, C=O_{HCOO} = 1.26 Å. Angle(s): all OC–Fe–CO = 90° ($Fe_2(CO)_6$ taken as bioctahedral fragment, local C_{2v} symmetry), all Fe–C–O = 180°, dihedral angle between $Fe_2C_3H_3$ plane and Fe_2S plane 90°, C–C–C in C_3H_3 bridge 115.4°, C–O–H = 120°. The HCOO group has 120° angles around C. H atoms and substituents of the C_3H_3 bridge are located on Fe–C–C and C–C–C bisector planes, oriented as in the structure of **5a**, and the S–H bond is equatorial or *exo* with respect to the bicyclo[3.1.0]-C_3Fe_2S frame).

Standard *in Situ* Preparation of Li[(μ-CO)(μ-RS)$Fe_2(CO)_6$]. A 250-mL Schlenk flask (one-necked, round bottomed) equipped with a stirbar and rubber septum was charged with 1.51 g (3.00 mmol) of $Fe_3(CO)_{12}$ and degassed via three evacuation/nitrogen-backfill cycles. The flask was then charged with 30 mL of THF by syringe, and the resulting deep green solution was cooled to −78 °C by immersing the flask in a dry ice/acetone slush bath. Subsequently, 3.00 mmol of the appropriate thiol was added by syringe, followed by the slow addition of 3.00 mmol of *n*-butyllithium also by syringe. The mixture was stirred for 10 min at −78 °C and then warmed to room temperature, during which time a green to brown-red color change was observed. The Li[(μ-CO)(μ-RS)$Fe_2(CO)_6$] reagent solution was stirred an additional 15 min at room temperature and subsequently used *in situ* without further purification.

Reaction of Li[(μ-CO)(μ-*t*-BuS)$Fe_2(CO)_6$] with Ethoxyacetylene. (a) Acetyl Chloride Quench. To the standard Li[(μ-CO)(μ-*t*-BuS)$Fe_2(CO)_6$] reagent solution (1.00 mmol) was added 0.09 mL (1.00 mmol) of ethoxyacetylene by syringe at room temperature. After the reaction mixture had been stirred for 30 min at room temperature, 0.11 mL (1.50 mmol) of acetyl chloride was added by syringe. Within minutes, a color change to cherry red occurred. After the mixture had been stirred for an additional 3.5 h, the solvent was removed *in vacuo* to yield a red solid, which was purified by filtration chromatography. Pentane eluted a minor pale orange band, which was not collected. Pentane/CH_2Cl_2 (3/2 v/v) eluted a dark orange band which gave 0.41 g (0.79 mmol, 79%) of (μ-EtOC=C(H)C-(OC(O)Me)=)(μ-*t*-BuS)$Fe_2(CO)_6$ (**5a**) as an air-stable, red solid, mp 111.0–113.0 °C after recrystallization from pentane/CH_2Cl_2.

Anal. Calcd for $C_{17}H_{18}Fe_2O_9S$: C, 40.03; H, 3.56. Found: C, 40.03; H, 3.55.

IR (CCl_4): 2960 w, 2940 w, 2890 w, 2860 vw, 1778 s (C=O), 1475 m, 1455 s, 1383 m, 1368 m, 1200 vs, 1155 vs, 1108 w, 1048 sh, 1020 vs, 850 w, 630 m, 610 s, 590 m, 490 w cm^{-1}; terminal carbonyl region (pentane) 2065 vs, 2025 vs, 2000 vs, 1990 vs, 1978 m, 1968 sh, 1948 vw cm^{-1}.

^{1}H NMR ($CDCl_3$; 250 MHz): δ 1.39 (s, 9H, SC(CH_3)), 1.42 (t, J = 6.89 Hz, 3H, OCH_2CH_3), 2.25 (s, 3H, C(O)CH_3), 4.07 (m, 2H, OCH_2CH_3), 6.85 (s, 1H, EtOC=C*H*).

^{13}C NMR ($CDCl_3$; 67.9 MHz): δ 14.06 (q, J = 128.1 Hz, OCH_2CH_3), 21.64 (q, J = 130.0 Hz, C(O)CH_3), 33.88 (q, J = 127.0 Hz, SC(CH_3)$_3$), 50.47 (s, S*C*(CH_3)$_3$), 71.56 (t, J = 148.0 Hz, OCH_2CH_3), 136.06 (d, J = 159.5 Hz, EtOC=*C*H), 165.37 (s, *C*(O)Me), 207.99, 210.12, and 214.20 (all s, Fe–CO), 267.43 (s, MeC(O)O*C*–CH), 284.82 (s, EtO*C*=CH).

(26) Pinhas, A. R.; Hoffmann, R. *Inorg. Chem.* **1979**, *18*, 654.

(27) (a) Hofmann, P.; Hämmerle, M.; Unfried, G. *New J. Chem.* **1991**, *15*, 769. (b) Albright, T. A.; Hoffmann, R.; Hofmann, P. *Chem. Ber.* **1978**, *111*, 1591.

(28) Ammeter, J. H.; Bürgi, H. B.; Thibeault, J. C.; Hoffmann, R. *J. Am. Chem. Soc.* **1978**, *100*, 3686.

(b) Benzoyl Chloride Quench. The same procedure was used, except that 0.37 mL (3.20 mmol) of benzoyl chloride was added. Over a period of several hours, a gradual color change to cherry red occurred. After the mixture had been stirred for a total of 18 h, the solvent was removed *in vacuo* to yield a red oil, which was purified by filtration chromatography. Pentane eluted a minor pale orange band, which was not collected. Pentane/CH_2Cl_2 (3/2 v/v) eluted a dark orange band, which gave 1.24 g (2.17 mmol, 71%) of (μ-EtOC=C(H)C(OC(O)Ph)=)(μ-*t*-BuS)$Fe_2(CO)_6$ (**5b**) as an air-stable, red solid, mp 115.0–118.0 °C after recrystallization from pentane/CH_2Cl_2.

Anal. Calcd for $C_{22}H_{20}Fe_2O_9S$: C, 46.18; H, 3.52. Found: C, 46.32; H, 3.55.

IR (CCl_4): 2975 m, 2940 w, 2930 w, 2900 w, 2870 w, 1748 vs (C=O), 1605 w (Ph), 1586 w (Ph), 1495 m, 1475 s, 1405 vs, 1385 s, 1368 m, 1310 w, 1225 vs, 1200 vs, 1190 s, 1160 s, 1110 m, 1078 m, 1040 vs, 1032 vs, 1000 vs, 980 s, 935 w, 850 w, 705 s, 687 w, 657 w, 632 m, 610 vs, 500 m cm^{-1}; terminal carbonyl region (pentane) 2065 vs, 2025 vs, 2000 vs, 1990 vs, 1980 s, 1975 sh, 1950 vw cm^{-1}.

^1H NMR (CD_2Cl_2; 300 MHz): δ 1.44 (s, 9H, $SC(CH_3)_3$), 1.44 (t, J = 7.52 Hz, 3H, OCH_2CH_3), 4.12 (m, 2H, OCH_2CH_3), 6.99 (s, 1H, EtOC=C*H*), 7.51–8.18 (m, 5H, C_6H_5).

^{13}C NMR ($CDCl_3$; 75.4 MHz): δ 14.18 (q, J = 127.8 Hz, OCH_2CH_3), 33.98 (q, J = 129.1 Hz, $SC(CH_3)_3$), 50.64 (s, $SC(CH_3)_3$), 71.69 (t, J = 147.7 Hz, OCH_2CH_3), 127.55–134.99 (m, C_6H_5), 136.16 (d, J = 159.8 Hz, EtOC=CH), 161.34 (s, C(O)Ph), 208.01, 208.20, 209.98, 210.10, 214.06, and 214.19 (all s, Fe–CO), 267.15 (s, PhC(O)OC–CH), 284.14 (s, EtO-C=CH).

Reaction of Li[(μ-CO)(μ-EtS)$Fe_2(CO)_6$] with Ethoxyacetylene. Acetyl Chloride Quench. To the standard Li[(μ-CO)(μ-EtS)$Fe_2(CO)_6$] reagent solution (2.73 mmol) was added 0.24 mL (2.73 mmol) of ethoxyacetylene by syringe at room temperature. After the reaction mixture had been stirred for 1 h at room temperature, 0.28 mL (4.00 mmol) of acetyl chloride was added by syringe. Within minutes, a color change to cherry red occurred. After the mixture had been stirred for an additional 16 h, the solvent was removed *in vacuo* to yield a red oil, which was purified by filtration chromatography. Pentane/CH_2Cl_2 (9/1 v/v) eluted two minor pale orange bands which were not collected. Pentane/CH_2Cl_2 (1/1 v/v) eluted a dark orange band which gave 0.98 g (2.04 mmol, 75%) of (μ-EtOC=C(H)C(OC(O)Me)=)(μ-EtS)$Fe_2(CO)_6$ (**5c**) as an air-stable, red solid, mp 108.0–110.0 °C, after recrystallization from pentane/CH_2Cl_2.

Anal. Calcd for $C_{15}H_{14}Fe_2O_9S$: C, 37.38; H, 2.93. Found: C, 37.52; H, 2.94.

IR (CCl_4): 2990 w, 2975 w, 2935 w, 2875 vw, 1780 vs (C=O), 1478 s, 1455 vs, 1385 s, 1370 s, 1278 w, 1255 w, 1205 vs, 1160 vs, 1110 m, 1095 w, 1050 s, 1025 vs, 850 m, 650 w, 630 s, 610 vs, 585 s, 500 m cm^{-1}; terminal carbonyl region (pentane) 2070 vs, 2030 vs, 2005 vs, 1995 vs, 1982 m, 1975 m, 1952 vw cm^{-1}.

^1H NMR (CD_2Cl_2; 300 MHz): δ 1.41 (t, J = 7.32 Hz, 3H, SCH_2CH_3), 1.42 (t, J = 6.98 Hz, 3H, OCH_2CH_3), 2.25 (s, 3H, $C(O)CH_3$), 2.57 (q, J = 7.44 Hz, 2H, SCH_2CH_3), 4.07 (m, 2H, OCH_2CH_3), 6.81 (s, 1H, EtOC=C*H*).

^{13}C NMR ($CDCl_3$; 67.9 MHz): δ 14.05 (q, J = 127.7 Hz, OCH_2CH_3), 18.57 (q, J = 128.3 Hz, SCH_2CH_3), 21.58 (q, J = 130.7 Hz, $C(O)CH_3$), 39.07 (t, J = 141.6 Hz, SCH_2CH_3), 71.46 (t, J = 146.8 Hz, OCH_2CH_3), 136.28 (d, J = 156.6 Hz, EtOC=CH), 165.23 (s, C(O)Me), 207.92, 208.08, 208.87, 208.97, and 214.15 (all s, Fe–CO), 266.07 (s, MeC(O)OC–CH), 283.76 (s, EtOC=CH).

Mass Spectrum (FD): *m/z* 482 (M^+).

Isolation of [Li(12-Crown-4)][(μ-EtOC=C(H)C(O)=)(μ-*t*-BuS)$Fe_2(CO)_6$]. To the standard Li[(μ-CO)(μ-*t*-BuS)Fe_2-$(CO)_6$] reagent solution (3.03 mmol) was added 0.26 mL (3.03mmol) of ethoxyacetylene by syringe at room temperature. After the reaction mixture had been stirred for 16 h at room temperature, the solvent was removed *in vacuo*. The resulting red, foamy solid was dissolved in Et_2O/CH_2Cl_2 (4/1 v/v) and this solution filtered under nitrogen into a 250-mL Schlenk flask equipped with a spinbar. To this solution was added 0.49 mL (3.03 mmol) of 12-crown-4 by syringe. Within minutes, a red precipitate had formed. After the reaction mixture had been stirred for 3 h at room temperature, the solvent was removed *in vacuo* to yield a red, foamy solid. This was dissolved in CH_2Cl_2/hexane (5 mL/4 mL) and filtered under nitrogen into a 50-mL Schlenk tube. Subsequent crystallization at −20 °C yielded 0.69 g (1.06 mmol, 35%) of [Li(12-Crown-4)][(μ-EtOC=C(H)C(O)=)(μ-*t*-BuS)$Fe_2(CO)_6$] (**6**).

Anal. Calcd for $C_{23}H_{31}Fe_2O_{12}SLi$: C, 42.49; H; 4.80. Found: C, 42.38; H, 4.87.

IR (CH_2Cl_2): 2990 sh, 2960 sh, 2930 s, 2880 s, 1465 sh, 1450 vs, 1420 s, 1390 w, 1362 m, 1160 sh, 1135 sh, 1125 vs, 1100 vs, 1055 m, 1025 s, 925 m, 860 m, 640 m, 610 s cm^{-1}.

^1H NMR (acetone-d_6; 300 MHz): δ 1.20 (t, J = 6.68 Hz, 3H, OCH_2CH_3), 1.33 (s, 9H, $SC(CH_3)_3$), 3.50 (m, 2H, OCH_2CH_3), 3.68 (s, 16H, $-OCH_2CH_2O-$), 5.27 (s, 1H, EtOC=C*H*).

^{13}C NMR (acetone-d_6; 67.9 MHz): δ 14.92 (q, J = 126.3 Hz, OCH_2CH_3), 34.57 (q, J = 126.0 Hz, $SC(CH_3)_3$), 38.42 (s, $SC(CH_3)_3$), 66.36 (t, J = 144.7 Hz, OCH_2CH_3), 68.89 (t, J = 143.5 Hz, $-OCH_2CH_2O-$), 125.52 (d, J = 147.6 Hz, EtOC=CH), 212.39, 213.05, 214.00 (broad), 219.76, 220.78 (all s, Fe–CO), 231.63 (s, EtOC=C(H)CO=), 259.78 (s, EtOC=CH).

Mass Spectrum (FAB): *m/z* 467 (M^- anion).

Mass Spectrum (FD): *m/z* 183 (M^+ cation).

Reaction of Li[(μ-CO)(μ-*t*-BuS)$Fe_2(CO)_6$] with Ethoxyacetylene. Trifluoroacetic Acid Quench. To the standard Li[(μ-CO)(μ-*t*-BuS)$Fe_2(CO)_6$] reagent solution (2.97 mmol) was added 0.26 mL (2.97 mmol) of ethoxyacetylene by syringe at room temperature. After the reaction mixture had been stirred for 30 min at room temperature, 0.23 mL (2.97 mmol) of trifluoroacetic acid was added by syringe. Within a few minutes, a color change to brighter red had occurred. After the mixture had been stirred for an additional 30 min, the solvent was removed *in vacuo* to yield a red solid, which was purified by filtration chromatography. Pentane eluted a yellow-brown band, which was not collected. Pentane/CH_2Cl_2 (9/1 v/v) eluted a dark orange band, which gave 1.05 g (2.24 mmol, 76%) of (μ-EtOC(=CH_2)C=O)(μ-*t*-BuS)$Fe_2(CO)_6$ (**7a**; a mixture of two inseparable isomers), as an air-stable, red solid, mp 76.5–78.0 °C, after recrystallization from pentane.

Anal. Calcd for $C_{15}H_{16}Fe_2O_8S$: C, 38.49; H, 3.44. Found: C, 38.75; H, 3.56.

IR ($CHCl_3$): 2990 s, 2965 s, 2942 s, 2922 s, 2900 m, 1600 s (C=C), 1482 vs (acyl C=O), 1470 sh, 1455 vs, 1441 s, 1390 m, 1378 m, 1361 vs, 1272 vs, 1151 vs, 1115 m, 1091 m, 1095 vs, 970 vs, 950 s, 850 s, 680 w, 620 vs, 608 vs cm^{-1}; terminal carbonyl region (pentane) 2072 s, 2034 vs, 2008 vs, 2000 vs, 1989 s, 1980 s cm^{-1}.

^1H NMR ($CDCl_3$; 250 MHz): δ 1.24 (s, 9H, $SC(CH_3)_3$ major isomer), 1.42 (t, J = 7.28 Hz, 3H, OCH_2CH_3 minor isomer), 1.45 (t, J = 7.10 Hz, 3H, OCH_2CH_3 major isomer), 1.54 (s, 9H, $SC(CH_3)_3$ minor isomer), 3.76 (m, 4H, OCH_2CH_3 both isomers), 3.84 (d, J = 2.26 Hz, 2H, $C=CH_2$ both isomers, diastereotopic CH_2), 4.32 (d, J = 2.25 Hz, 2H, $C=CH_2$ both isomers, diastereotopic CH_2). Ratio major/minor: 2.7/1.0.

^{13}C NMR ($CDCl_3$; 67.9 MHz): δ 13.86 (q, J = 127.0 Hz, OCH_2CH_3 both isomers), 34.23 (q, J = 125.7 Hz, $SC(CH_3)_3$ minor isomer), 34.82 (q, J = 127.4 Hz, $SC(CH_3)_3$ major isomer), 48.02 (s, $SC(CH_3)_3$ major isomer), 49.47 (s, $SC(CH_3)_3$ minor isomer), 64.04 (t, J = 142.2 Hz, OCH_2CH_3 both isomers), 84.66 (t, J = 161.6 Hz, $C=CH_2$ major isomer), 85.68 (t, J = 163.1 Hz, $C=CH_2$ minor isomer), 159.70 (s, $EtOC=CH_2$ both isomers), 207.26, 209.51, 210.37, 210.55, 210.72, and 211.21 (all s, Fe–CO), 287.24 (s, acyl C=O both isomers).

Mass Spectrum (EI): *m/z* (relative intensity) 468 (M^+, 8), 440 ($M^+ - CO$, 29), 412 ($M^+ - 2CO$, 28), 384 ($M^+ - 3CO$, 30), 356 ($M^+ - 4CO$, 38), 328 ($M^+ - 5CO$, 62), 300 ($M^+ - 6CO$, 100), 272 ($M^+ - 7CO$, 51), 244 (*t*-BuS$Fe_2HOC=CH_2$, 63), 216 ($HSFe_2EtOC=CH_2$, 82), 188 ($HSFe_2HOC=CH_2$, 60), 170 ($SFe_2C=CH_2$, 14), 159 ($SFeEtOC=CH_2$, 8), 145 (Fe_2SH, 55), 144 (Fe_2S, 56), 112 (Fe_2, 4), 57 (*t*-Bu, 27), 56 (Fe, 6).

Reaction of Li[(μ-CO)(μ-EtS)$Fe_2(CO)_6$] with Ethoxyacetylene. Trifluoroacetic Acid Quench. To the standard Li[(μ-CO)(μ-EtS)$Fe_2(CO)_6$] reagent solution (3.02 mmol) was added 0.26 mL (3.02 mmol) of ethoxyacetylene by syringe at room temperature. After the reaction mixture had been stirred for 30 min at room temperture, 0.23 mL (3.02 mmol) of trifluoroacetic acid was added by syringe. After the mixture had been stirred for an additional 1 h, the solvent was removed *in vacuo* to yield a red-brown, oily solid, which was purified by filtration chromatography. Hexane eluted a minor pale orange band, which was not collected. Further elution with hexane gave an orange band which produced 0.42 g (1.01 mmol, 34%) of (μ-η^1:η^2-EtOC=CH_2)(μ-EtS)$Fe_2(CO)_6$ (**8b**) as a slightly air sensitive red oil.

Anal. Calcd for $C_{12}H_{12}Fe_2O_7S$: C, 34.98; H, 2.94. Found: C, 35.27; H, 3.00.

IR (CCl_4): 3060 vw, 2980 sh, 2960 m, 2930 s, 2870 m, 2860 sh, 1460 sh, 1458 s, 1390 sh, 1380 m, 1280 s, 1255 m, 1150 vs, 1108 w, 1028 s, 955 m, 900 m, 840 w, 670 m, 620 vs, 600 s, 570 s cm^{-1}; terminal carbonyl region (pentane) 2070 s, 2050 vw, 2040 vs, 2000 vs, 1900 vs cm^{-1}.

^{1}H NMR ($CDCl_3$; 300 MHz): δ 1.26 (t, J = 6.73 Hz, 3H, OCH_2CH_3), 1.30 (t, J = 7.24 Hz, 3H, SCH_2CH_3), 1.65 (d, J = 4.61 Hz, 1H, C=CH_2*endo*), 2.38 (m, 1H, SCH_2CH_3, diastereotopic CH_2), 2.41 (m, 1H, SCH_2CH_3, diastereotopic CH_2), 3.21 (d, J = 4.61 Hz, 1H, C=CH_2*exo*), 3.64 (m, 1H, OCH_2CH_3, diastereotopic CH_2), 3.85 (m, 1H, OCH_2CH_3, diastereotopic CH_2).

^{13}C NMR ($CDCl_3$; 67.9 MHz): δ 14.39 (q, J = 127.3 Hz, OCH_2CH_3), 18.16 (q, J = 126.1 Hz, SCH_2CH_3), 33.59 (t, J = 144.6 Hz, SCH_2CH_3), 49.01 (dd, J = 152.0 Hz, J = 161.9 Hz, C=CH_2), 66.79 (t, J = 146.8 Hz, OCH_2CH_3), 209.42 and 209.97 (both s, Fe—CO), 218.02 (s, EtO*C*=CH_2).

Mass Spectrum (EI): *m/z* (relative intensity) 412 (M^+, 13), 384 (M^+ − CO, 24), 356 (M^+ − 2CO, 33), 328 (M^+ − 3CO, 41), 300 (M^+ − 4CO, 28), 272 (M^+ − 5CO, 63), 244 (M^+ − 6CO, 100), 216 ($HSFe_2EtOC{=}CH_2$, 67), 188 ($HSFe_2HOCCH_2$, 63), 145 ($HSFe_2$, 48), 144 (SFe_2, 54), 112 (Fe_2, 7), 69 (EtOC=C, 5), 56 (Fe, 7).

Further elution with hexane then yielded a minor dark green band, which was not collected, and a dark orange band, which gave 0.70 g (1.60 mmol, 53%) of (μ-EtOC(=CH_2)C=O)-(μ-EtS)$Fe_2(CO)_6$ (**7b**; a mixture of inseparable isomers) as a slightly air sensitive red oil. An analytically pure sample for carbon/hydrogen combustion analysis could not be obtained.

IR (CCl_4): 2980 sh, 2960 vs, 2945 vs, 2870 s, 2850 s, 1600 s (C=C), 1480 vs (acyl C=O), 1455 s, 1378 s, 1358 m, 1280 vs, 1258 s, 1151 s, 1117 m, 1091 m, 1061 vs, 1028 m, 975 vs, 950 sh, 900 w, 872 w, 848 m, 710 m, 695 m, 682 m, 630 vs, 610 vs, 590 vs cm^{-1}; terminal carbonyl region (pentane) 2075 s, 2040 vs, 2000 vs, 1992 sh, 1981 m, 1975 sh cm^{-1}.

^{1}H NMR (CD_2Cl_2; 300 MHz): δ 1.31 (t, J = 7.30 Hz, 3H, SCH_2CH_3 minor isomer), 1.42 (t, J = 7.14 Hz, 3H, OCH_2CH_3 major isomer), 1.44 (t, J = 7.11 Hz, 3H, OCH_2CH_3 minor isomer), 1.49 (t, J = 6.81 Hz, 3H, SCH_2CH_3 major isomer), 2.11, 2.22, and 2.64 (all m, 4H, SCH_2CH_3 both isomers), 3.77 (m, 4H, OCH_2CH_3 both isomers), 3.86 (d, J = 1.73 Hz, 1H, C=CH_2 minor isomer, diastereotopic CH_2), 3.88 (d, J = 2.50 Hz, 1H, C=CH_2 major isomer, diastereotopic CH_2), 4.31 (d, J = 2.50 Hz, 1H, C=CH_2 major isomer, diastereotopic CH_2), 4.35 (d, J = 1.58 Hz, 1H, C=CH_2 minor isomer, diastereotopic CH_2). Ratio major/minor: 1.8/1.0.

^{13}C NMR ($CDCl_3$; 67.9 MHz): δ 13.87 (q, J = 127.5 Hz, OCH_2CH_3 both isomers), 17.78 (q, J = 128.4 Hz, SCH_2CH_3 minor isomer), 18.28 (q, J = 128.6 Hz, SCH_2CH_3 major isomer), 25.56 (t, J = 141.5 Hz, SCH_2CH_3 minor isomer), 32.69 (t, J = 140.8 Hz, SCH_2CH_3 major isomer), 64.06 (t, J = 144.0 Hz, OCH_2CH_3 both isomers), 84.03 (t, J = 162.6 Hz, C=CH_2 minor isomer), 85.22 (t, J = 162.7 Hz, C=CH_2 major isomer), 160.14 (s, EtO*C*=CH_2 major isomer), 160.58 (s, EtO*C*=CH_2 minor isomer), 207.88, 209.31, 209.77, 210.19, 210.40, and 211.03 (all s, Fe—CO), 287.64 (s, acyl C=O major isomer), 290.03 (s, acyl C=O minor isomer).

Mass Spectrum (EI): *m/z* (relative intensity) 440 (M^+, 1), 412 (M^+ − CO, 16), 384 (M^+ − 2CO, 19), 356 (M^+ − 3CO, 28), 328 (M^+ − 4CO, 36), 300 (M^+ − 5CO, 33), 272 (M^+ − 6CO, 68), 244 (M^+ − 7CO, 100), 216 ($HSFe_2EtOC{=}CH_2$, 65), 188 ($HSFe_2HOC{=}CH_2$, 66), 169 ($HSFe_2C{=}C$, 9), 145 (Fe_2SH, 66), 144 (Fe_2S, 65), 112 (Fe_2, 9), 56 (Fe, 8).

Decarbonylation of (μ-EtOC(=CH_2)C=O)(μ-*t*-BuS)$Fe_2(CO)_6$. A 100-mL round-bottomed flask equipped with a stirbar and rubber septum was charged with 0.34 g (0.72 mmol) of (μ-EtOC(=CH_2)C=O)(μ-*t*-BuS)$Fe_2(CO)_6$ (**7a**) and degassed via three evacuation/nitrogen-backfill cycles. The flask then was charged with 30 mL of THF by syringe. After the resulting red reaction mixture had been stirred for 6 days at room temperature, the solvent was removed *in vacuo* to yield a red oil, which was purified by filtration chromatography. Pentane eluted a red band, which gave 0.29 g (0.67 mmol, 92%) of (μ-η^1:η^2-EtOC=CH_2)(μ-*t*-BuS)$Fe_2(CO)_6$ (**8a**), identified by its ^{1}H NMR spectrum.[1]

Decarbonylation of (μ-EtOC(=CH_2)C=O)(μ-EtS)$Fe_2(CO)_6$. A similar procedure was used in the decarbonylation of 0.41 g (0.93 mmol) of (μ-EtOC(=CH_2)C=O)(μ-EtS)$Fe_2(CO)_6$ (**7b**) (4-day reaction time). A red oil was obtained, which was purified by filtration chromatography. Pentane eluted an orange band, which gave 0.36 g (0.88 mmol, 95%) of (μ-η^1:η^2-EtOC=CH_2)(μ-EtS)$Fe_2(CO)_6$ (**8b**), identified by its ^{1}H NMR spectrum.

Low-Temperature Reaction of Li[(μ-CO)(μ-*t*-BuS)$Fe_2(CO)_6$] with Ethoxyacetylene. Trifluoroacetic Acid Quench. To the standard Li[(μ-CO)(μ-*t*-BuS)$Fe_2(CO)_6$] reagent solution (1.58 mmol) cooled to −78 °C was added 0.14 mL (1.58 mmol) of ethoxyacetylene by syringe. After the reaction mixture had been stirred for 1 h at −78 °C, 0.12 mL (1.80 mmol) of trifluoroacetic acid was added by syringe. After the mixture had been stirred for an additional 15 min at −78 °C, warmed to room temperature, and stirred for 15 min at room temperature, the solvent was removed *in vacuo* to yield a red tar, which was purified by filtration chromatography. Pentane eluted a dark orange band, which gave 0.40 g (0.92 mmol, 58%) of (μ-η^1:η^2-EtOC=CH_2)(μ-*t*-BuS)$Fe_2(CO)_6$ (**8a**), identified by its ^{1}H NMR spectrum.[1] Further elution with pentane yielded a minor pale green band, which was not collected, and a pale orange band, which gave 0.13 g (0.27 mmol, 17%) of (μ-EtOC(=CH_2)C=O)(μ-*t*-BuS)$Fe_2(CO)_6$ (**7a**), also identified by its ^{1}H NMR spectrum.

Acknowledgment. We are grateful to the National Science Foundation (D.S.) and to the Volkwagen-Stiftung and Fonds der Chemischen Industrie (P.H.) for support of this work. This MIT/TU München collaboration was made possible by a Senior Award within the Sonderprogramm für Naturwissenschaftler aus den Vereinigten Staaten von Amerika of the Alexander von Humboldt-Stiftung to D.S., which is gratefully acknowledged.

OM9400356